Journal of Naval Sciences and Engineering

Deniz Bilimleri ve Mühendisliği Dergisi

Barbaros Naval Sciences and Engineering Institute
Barbaros Deniz Bilimleri ve Mühendisliği Enstitüsü

Volume/Cilt:16
Number/Sayı:1
April/2020

PRINTED BY/BASKI
Turkish Naval Academy Printing House/Deniz Harp Okulu Basımevi

CORRESPONDENCE AND COMMUNICATION ADDRESS/YAZIŞMA VE HABERLEŞME ADRESİ

Milli Savunma Üniversitesi
Barbaros Deniz Bilimleri ve Mühendisliği Enstitüsü
Deniz Harp Okulu Yerleşkesi
Tuzla/İSTANBUL/TÜRKİYE

Phone/Telefon : +90 216 395 26 30
Fax/Belgegeçer : +90 216 395 26 58
E-mail/E-posta : jnse@dho.edu.tr
Web : http://www.dergipark.gov.tr/jnse

NATIONAL DEFENSE UNIVERSITY
BARBAROS NAVAL SCIENCES AND ENGINEERING INSTITUTE
JOURNAL OF NAVAL SCIENCES AND ENGINEERING

MİLLİ SAVUNMA ÜNİVERSİTESİ
BARBAROS DENİZ BİLİMLERİ VE MÜHENDİSLİĞİ ENSTİTÜSÜ
DENİZ BİLİMLERİ VE MÜHENDİSLİĞİ DERGİSİ

Volume/Cilt: 16 Number/Sayı: 1 April/Nisan 2020 ISSN: 1304-2025

Owner on Behalf of the Barbaros Naval Sciences and Engineering Institute
Barbaros Deniz Bilimleri ve Mühendisliği Enstitüsü Adına Sahibi ve Sorumlusu
Assoc.Prof.Dr. (Doç.Dr.) Ertan YAKICI

Journal of Naval Sciences and Engineering is a peer reviewed, international, inter-disciplinary journal in science and technology, which is published semi-annually in April and November since 2003. It publishes full research articles, review articles, technical notes, short communications, book reviews, letters to the editor and extended versions of conference papers. Topics of interest include the technological and scientific aspects of the following areas: **Computer Science and Engineering**, **Electrical and Electronics Engineering**, **Naval/Mechanical Engineering**, **Naval Architecture and Marine Engineering, Industrial Engineering and Basic/Social Sciences**. The journal aims to provide a scientific contribution to the increasing needs of Turkish Armed Forces. The papers in the journal are published in English.

Following Open Access Model of Publishing, Journal of Naval Sciences and Engineering presents a variety of scientific viewpoints. The authors are responsible for the scientific, contextual and linguistic aspects of the articles published in the journal. The views expressed or implied in this publication, unless otherwise noted, should not be interpreted as official positions of the Institution.

Our journal uses double-blind review, which means that both the reviewer and author identities are concealed from the reviewers, and vice versa, throughout the review process. The articles submitted to JNSE to be published are free of article submission, processing and publication charges. The accepted articles are published free-of-charge as online from the journal website and printed.

DATABASES INDEXING OUR JOURNAL / TARANDIĞIMIZ VERI TABANLARI

Open Academic Journals Index (OAJI) (13.03.2016)
Sobiad Citation Index (31.01.2018)
Scientific Indexing Services (SIS) (28.02.2018)
Arastirmax Scientific Publication Index (13.03.2018)
CiteFactor Academic Scientific Journals (14.05.2018)
Asian Digital Library (03.09.2018)
Idealonline (05.09.2018)
Directory of Open Access Journals (DOAJ) (09.10.2018)

Deniz Bilimleri ve Mühendisliği Dergisi; uluslararası düzeyde, hakemli, çok disiplinli, Nisan ve Kasım aylarında olmak üzere 2003 yılından bu yana yılda iki kez yayımlanan, bilim ve teknoloji dergisidir. Dergide; Bilgisayar, Makine, Gemi İnşa, Elektrik/Elektronik, Endüstri Mühendisliği ile Temel ve Sosyal Bilimler alanlarında bilimsel nitelikli araştırma makaleleri, derlemeler, teknik notlar, kitap incelemeleri, editöre mektuplar ile konferans ve toplantıların genişletilmiş raporlarına yer verilmektedir. Dergi, Türk Silahlı Kuvvetlerinin artan ihtiyaçlarına bilimsel katkı sağlamayı amaçlamaktadır. Dergide yer alan makaleler İngilizce olarak yayımlanmaktadır.

Açık erişimli yayın politikası izleyen Deniz Bilimleri ve Mühendisliği Dergisi değişik bilimsel bakış açılarını okuyucularına sunmaktadır. Dergide yayınlanan makalelerin bilim, içerik ve dil bakımından sorumluluğu yazarlarına aittir. Doğrudan veya dolaylı olarak ifade edilen görüşler kurumun resmi görüşleri olarak görülmemelidir.

Dergimiz, makale değerlendirme sürecinde çift-kör hakemlik sistemini kullanmaktadır. DBMD'ye yayımlanmak üzere gönderilen makaleler; makale gönderim, işlem ve yayın ücretinden muaftır. Kabul edilen makaleler, ücretsiz olarak basılı şekilde ve dergi web sayfasından çevrimiçi (on-line) olarak yayınlanmaktadır.

NATIONAL DEFENSE UNIVERSITY
BARBAROS NAVAL SCIENCES AND ENGINEERING INSTITUTE
JOURNAL OF NAVAL SCIENCES AND ENGINEERING

MİLLİ SAVUNMA ÜNİVERSİTESİ
BARBAROS DENİZ BİLİMLERİ VE MÜHENDİSLİĞİ ENSTİTÜSÜ
DENİZ BİLİMLERİ VE MÜHENDİSLİĞİ DERGİSİ

Volume/Cilt: 16 Number/Sayı: 1 April/Nisan 2020 ISSN: 1304-2025

NATIONAL DEFENSE UNIVERSITY
BARBAROS NAVAL SCIENCES AND ENGINEERING INSTITUTE
JOURNAL OF NAVAL SCIENCES AND ENGINEERING

VOLUME: 16 NUMBER: 1 APRIL 2020 ISSN: 1304-2025

CONTENTS / İÇİNDEKİLER

MİLLİ SAVUNMA ÜNİVERSİTESİ
BARBAROS DENİZ BİLİMLERİ VE MÜHENDİSLİĞİ ENSTİTÜSÜ
DENİZ BİLİMLERİ VE MÜHENDİSLİĞİ DERGİSİ

CİLT: 16 SAYI: 1 NİSAN 2020 ISSN: 1304-2025

Journal of Naval Sciences and Engineering
2020, Vol. 16, No.1, pp.1-24
Mechanical Engineering/Makine Mühendisliği

RESEARCH ARTICLE

DESING AND ANALYSIS OF AN AXIAL COMPRESSOR FOR A TURBOFAN ENGINE

Doğuş ÖZKAN[1]
Kadir BÜYÜKHAMURKAR[2]

[1]*National Defence University, Turkish Naval Academy, Mechanical Engineering, Istanbul, Turkey,*
dozkan@dho.edu.tr; ORCID: 0000-0002-3044-4310

[2] *Turkish Navy, Istanbul, Turkey,*
kbuyukhamurkar@gmail.com; ORCID: 0000-0001-8902-4604

Date of Receive: 04.03.2020 **Date of Acceptance: 20.04.2020**

ABSTRACT

Turbofan engines are used to provide thrust force by using the high temperature and pressure gases flow from the nozzle to move passenger planes or war jet planes. Turbofan engines consist of complicated parts such as axial fan, compressor, combustion chamber, turbine, which are manufactured with high engineering knowledge. Therefore, it needs to be well designed, analyzed and manufactured. In this study, an axial compressor of a warplane turbofan engine was designed and analyzed with AxStream software. Results were compared with real turbofan engine measured values, furthermore, computed flued dynamic and strain analysis were performed to evaluate compressor design parameters. Results showed that the polyprotic efficiency of the designed compressor was 2 % higher than the actual compressor. Furthermore, similar pressure and temperature were obtained at the outlet of the designed compressor.

Keywords: *Turbofan Engine, AxStream, Axial Compressor, Computed Fluid Dynamics.*

TURBOFAN MOTOR İÇİN EKSENEL AKIŞLI KOMPRESÖR TASARIMI VE ANALİZİ

ÖZ

Turbofan motorları, yolcu uçaklarını veya savaş jet uçaklarını hareket ettirmek için nozülden gelen yüksek sıcaklık ve basınç gazlarını kullanarak itme kuvveti sağlamak için kullanılır. Turbofan motorları, yüksek mühendislik bilgisi ile üretilen eksenel fan, kompresör, yanma odası, türbin gibi karmaşık parçalardan oluşur. Bu nedenle, iyi tasarlanmış, analiz edilmiş ve üretilmiş olmalıdır. Bu çalışmada, bir savaş uçağı turbofan motorunun eksenel kompresörü AxStream yazılımı ile tasarlanmış ve analiz edilmiştir. Sonuçlar gerçek turbofan motor ölçüm değerleri ile karşılaştırılmış, ayrıca kompresör tasarım parametrelerini değerlendirmek için hesaplamalı akışkan dinamiği ve gerilme analizi yapılmıştır. Sonuçlar, tasarlanan kompresörün poliprotik verimliliğinin gerçek kompresörden % 2 daha yüksek olduğunu göstermiştir. Ayrıca, tasarlanan kompresörün çıkışında gerçek kompresör göre benzer basınç ve sıcaklık elde edilmiştir.

Anahtar Kelimeler: *Turbofan Motor, AxStream, Eksenel Kompresor, Hesaplamalı Akışkan Dinamiği.*

NOMENCLATURE

Lu : Specific work coefficient

U : Rotor speed

Lu_z : Specific work gradient

H : Head of the compressor

h : Entalphy

w : Relative velocity

p : Pressure

γ, φ : Stator/rotor velocity coefficient

$\dot{m}$: Mass flow rate

ρ : Density

$\overline{w}$: Total pressure loss coefficient

c : Absolute velocity

A : Area

s : Entrophy

$\overline{w_N}$: Pressure loss coefficient of stator

$\overline{w_R}$: Pressure loss coefficient of rotor

$p_2 = P(h_2, s_2)$: Pressure function

$s_1 = S(p_1, h_1)$ **:** Entropy function

β **:** Flow angle in relative frame

1. INTRODUCTION

Turbojet engine has been started to use in aviation since 1941 by the invention of Franks Whittle [1]. The first turbojet engine consisted of a radial compressor, a single combustion chamber, turbine and it was a water-cooled engine [2]. Besides, turbo jet engines were modified and different kinds of engines have been manufactured such as turbo prob and turbofan that used in aviation [3]. Turbofan engines are the most commonly used aircraft propulsion both in civil and military aviation applications which has a large fan driven by turbine mechanical energy and a large amount of airflow through a duct around the engine [4]. The main parts of these engines axial fan, compressor, combustion chamber, turbine and nozzle [5]. Axial fan compresses the air which its pressure and temperature increase before entering the axial compressors [6]. Axial flow compressor increase, not only pressure but also the temperature of the air as a consequence of a given pressure ratio by changing the velocity and also enthalpy of the air [7, 8]. Axial compressors consist of stages in which one stage is formed by one stator and rotor blades [9]. Furthermore, compressor stage numbers can be up to 20 stages. The computer-aided design of an axial compressor has been the most common method with advance calculations. On the other hand, design can be analyzed by advanced techniques such as computed fluid dynamic (CFD) and strain analysis [10-12]. This study presents a novel approach to improve and compare an actual compressor performance that runs in warplanes by using advanced software. Therefore, AxStream software (manufactured by Softinway company) was used to design and analysis of 5 stages of an axial compressor by using compressor running parameters of a turbofan engine of a jet fighter in this study. Design and analysis results were compared to running parameters of this turbofan engine. Results showed that the design pressure of air at the exit of the compressors was % 93 similar to the real engine pressure value.

2. MATERIALS AND METHODS

The main design parameters of the axial compressor for the turbofan engine can be seen in Table 1. The axial compressor was considered to consist of 5 stages and inlet temperature, the pressure was the out of the fan flow.

Table 1. Design parameters.

Inputs	**Units**	**Minimum**	**Maximum**
Inlet pressure	kPa	426.32	426.32
Inlet temperature	K	475	475
Total outlet pressure	kPa	2643.21	2643.21
Mass flow	kg/s	52.89	52.89
Inlet flow angle	tan.deg	90	90
Inlet guide vane outlet angle	tan.deg	70	70
Shaft rotation	rpm	22800	22800
Mean diameter	mm	450	600
1'st blade height	mm	50	80
Work coefficient (Lu/U_2^2)	-	0.1	0.5
Specific work gradient (Lu_z/Lu_1)	-	0.1	0.5
Stage number	-	1	5
Hub diameter	mm	1.0	10000

The following fundamental energy, continuity and work equations were used to calculate the design outputs of the axial compressor, respectively [13]. Eq. 1 shows energy transfer per mass in an adiabatic flow that occurs in a rotating wheel with the angular speed of ω. $\dot{m}$ in Eq. 4 is the continuity downstream of the working wheel.

$$H = h + \frac{w^2 - U^2}{2} \tag{1}$$

$$s_0 = S\left(p, \frac{1}{\gamma^2}\left(h - (1-\gamma^2)h_{0_w^*}\right)\right) \tag{2}$$

$$s_0 = S\left(\frac{p_R^* - \bar{w}p_0}{1-\bar{w}}, \qquad h_R^* - \frac{U^2}{2} + \frac{U_0^2}{2}\right) \tag{3}$$

$$\dot{m} = \rho(p_2, h_2).w_2.\sin\beta_2.A_2 \tag{4}$$

$$H = h_1 + \frac{c_1^2}{2} - U_1 c_{1u} \tag{5}$$

$$p_1 = P\left(h_0^* - \frac{c_1^2}{2\varphi^2}, s_0^*\right) \tag{6}$$

$$h_1 = h_0^* - \frac{c_1^2}{2} \tag{7}$$

$$s_1 = S(p_1, h_1) \tag{8}$$

$$h_2 = H + \frac{c_2^2}{2} - \frac{W_2^2}{2} \tag{9}$$

$$s_2 = S\left(P\left(H + \frac{U_2^2}{2} - \overline{w_w}(p_{1_R}^* - p_1)\right), s_1\right) \tag{10}$$

$$p_2 = P(h_2, s_2) \tag{11}$$

$$h_3 = h_2^* - \frac{c_3^2}{2} \tag{12}$$

$$s_3 = S(p_2^* - \overline{w_N}(p_2^* - p_2), h_2^*) \tag{13}$$

$$p_2 = P(h_3, s_3) \tag{14}$$

From the known velocity coefficients of φ, γ or total pressure coefficient $\overline{w_w}$, $\overline{w_N}$ three equation that is shown in Eq. 15, 16 and 17 can be derived for the compressor stage.

$$k_2(\dot{m}, w_2) = 0 \tag{15}$$

$$k_3(\dot{m}, w_2, c_3) = 0 \tag{16}$$

$$k_0(\dot{m}, w_2, c_3) = 0 \tag{17}$$

AxStream software solves numerically by minimizing of $k_2^2 + k_3^2 + k_0^2$ by a method of conjugated gradients. Here 2000 iteration was used to find the best solution to these equations with the residual target set to 3.0e–5 (=RMS). Results, such as efficiency, main dimensions, temperature, pressure, and power, were compared to real engine design and running parameters. Furthermore, 3D aerodynamic and stress calculations were performed to improve the design.

3. RESULT AND DISCUSSION

3.1. Main Design and Flow Results

The optimum main dimensions of the designed 5 stages axial compressor is shown in Fig. 1(a) with % 87.9 total efficiency. The average compressor diameter was found to be 422.19 mm and the inlet guide vane height was 60.87 mm whereas the first stage rotor and stator blade height was found 48.49, 46.48 mm, respectively. The designed compressor 3D view was shown in Fig. 1(b). Furthermore, the enthalpy-entropy diagram in Fig. 1(c)

set out an enthalpy increase in the compressor which higher at the rotor blades than the stator blades. 1D and 2D streamline calculations are shown in Fig. 2, where inlet pressure was increased from 423 kPa to 2690 kPa and the total temperature at the exit increased to 835 K. Furthermore, inlet total enthalpy and total air velocity increased from 478 kj/kg to 885 kj/kg and 248.3 m/s to 457.9 m/s.

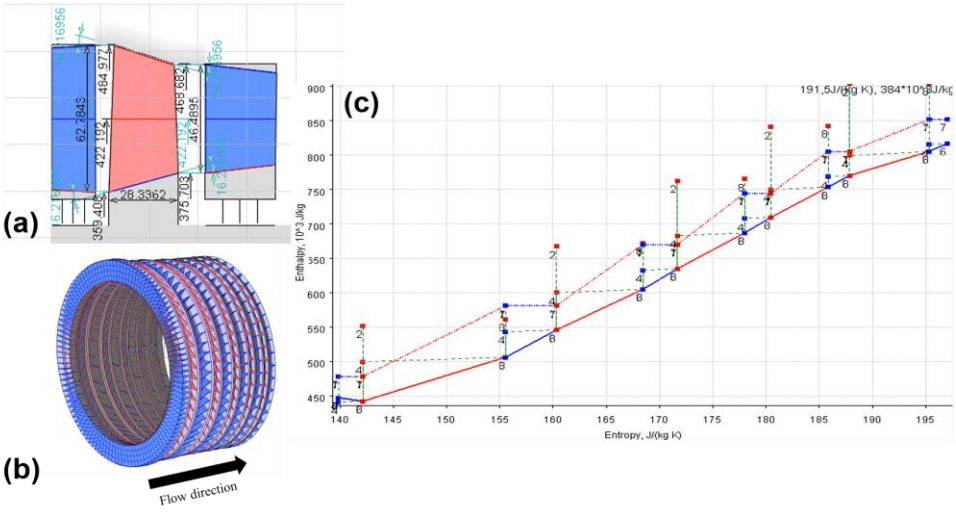

Figure 1. (a) 5 stages axial compressor with dimensions and inlet guide vanes (red blades are the rotor and blue ones are stator blades), (b) 3D image of the designed compressor, (c) enthalpy-entropy diagram of the designed compressor.

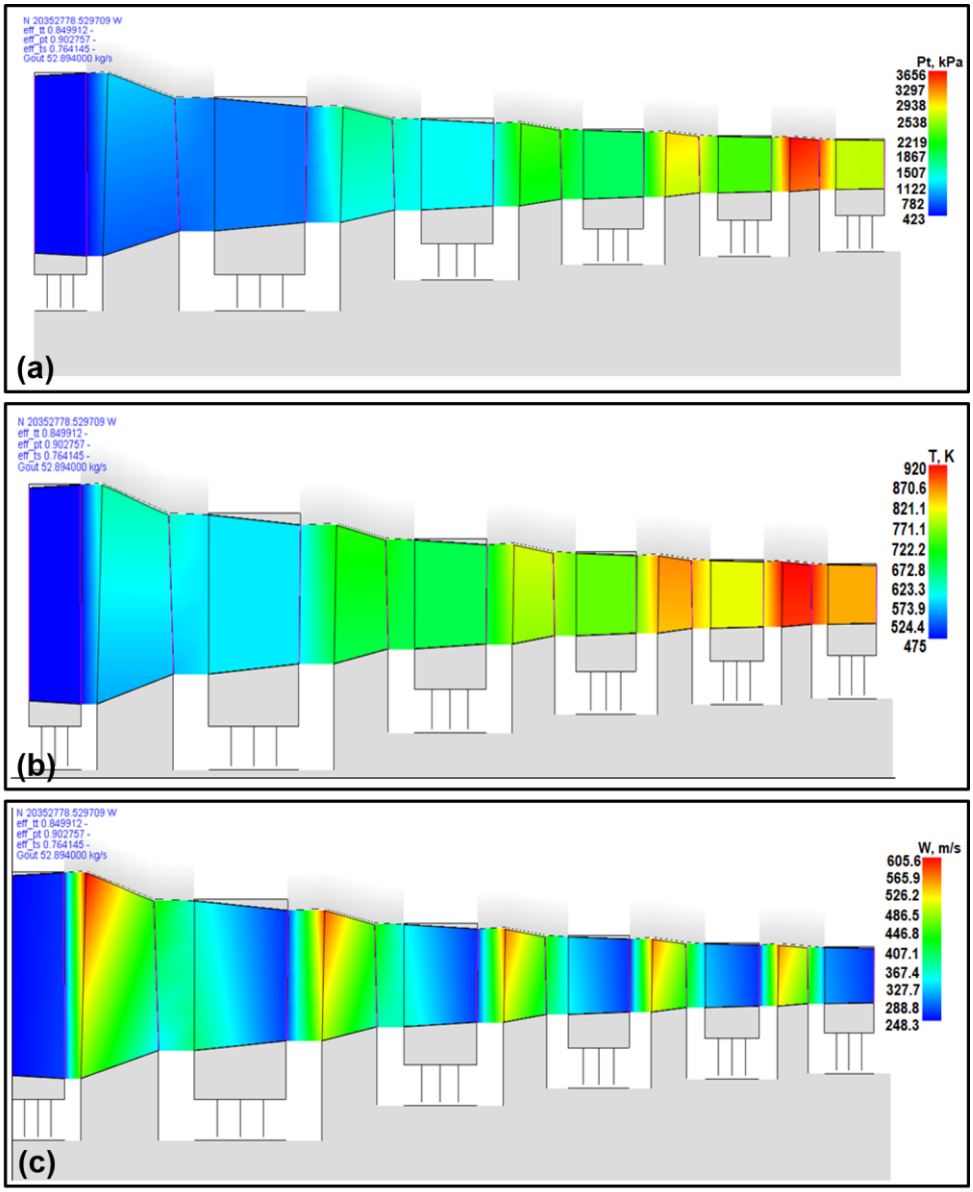

Figure 2. 1 and 2D flow calculations of axial compressor, (a) total pressure, (b) total temperature, (c) total velocity increase of the air at stages.

3.2. Stage Analysis of the Compressor

In this section, detailed enthalpy, pressure, stress, velocity and computational fluid dynamic analysis (CFD) analysis of each stage of the axial compressor were evaluated. Vectorial velocity diagrams are shown with velocities and angles where *A* is the angle between angular and absolute velocity, B is the angle between angular and relative velocity, C is the absolute velocity, K1, K2 denotes inlet and outlet air angle of air according to the blade.

3.2.1. Inlet Guide Vanes (IGV)

The calculated absolute velocities and angles are shown in Fig. 3 in where C_{in} and C_{out} were 248.3 m/s and 268.58 m/s. In addition, A and B were 90° whereas K1 and K2 were determined to be 90° and 68.46°, respectively (see Fig. 3 (a)).

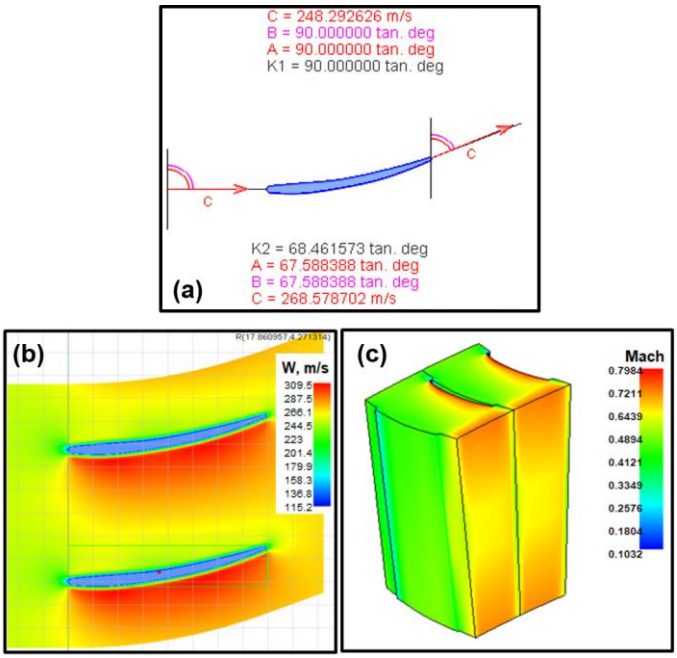

Figure 3. (a) absolute velocity and angles of the IGV, (b) relative velocity change at IGVs, (c) Mach number change of flow at IGVs.

A significant relative velocity increase was observed at the pressure sides of the IGVs due to the separation of the airflow from the blade surface (see Fig. 3(b)). Meanwhile, the exit IGV average Mach number was determined to be 0.72 which was in the range of 0.7-1.1 for aerospace application gas turbines [14]. However, the increase in the relative velocity due to the flow separation also increased the Mach number to 0.79 (see Fig. 3(c)).

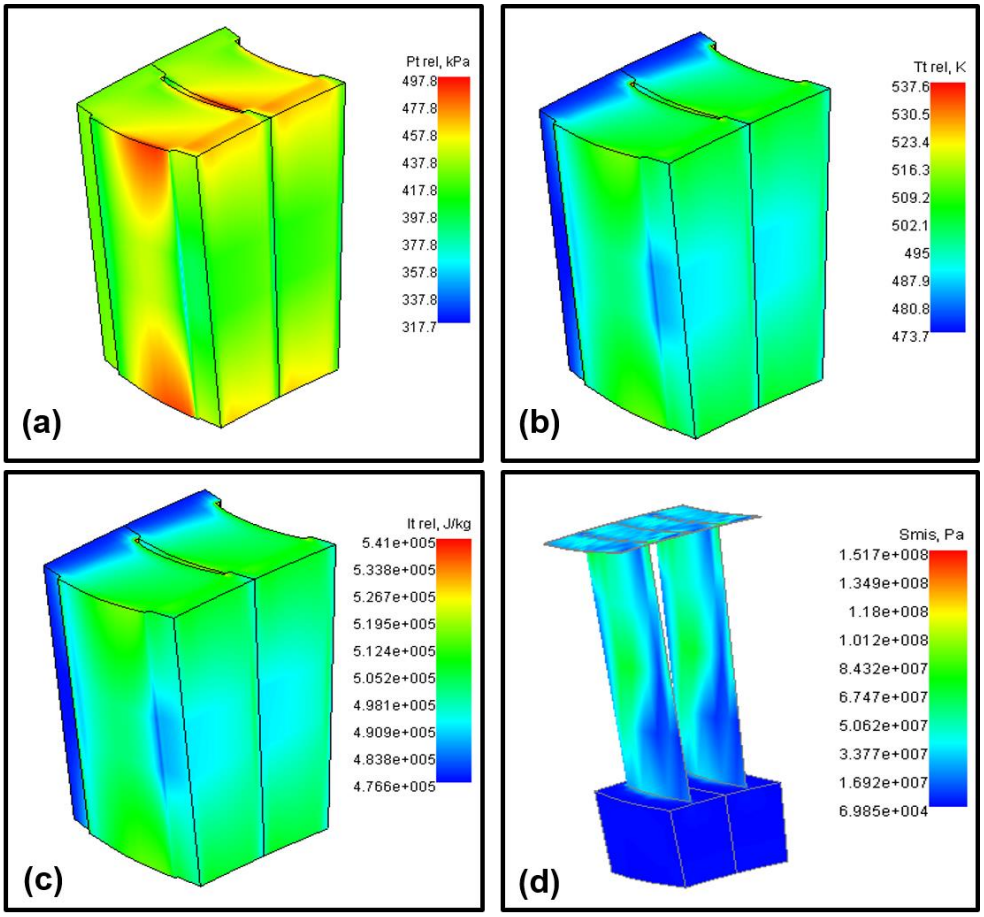

Figure 4. CFD analysis of the IGV flow, (a) total pressure, (b) total temperature, (c) total enthalpy change, (d) stress analysis of IGV blade.

The calculated average total pressure of 423 kPa was close to the design inlet pressure of the flow whereas, red areas in the flow indicate the highest total pressure of 461.5 kPa (see Fig. 4(a)). Furthermore, the highest total temperature was calculated to be 503 K while the average temperature was 487 K (see Fig. 4(b)). On the other hand, the average total enthalpy increased from 476.6 kj/kg to 506.3 kj/kg (see Fig. 4(b)). Moreover,

according to the Von Mises stress analysis, the maximum calculated stress was 97.12 MPa (see Fig.4(c)).

3.2.2. First Stage Analysis

Fig. 5 shows the first stage velocity triangles where the inlet absolute velocity *(C)* increased from 268.58 m/s to 387.64 m/s at the exit. Meanwhile, inlet rotor relative velocity *(W)* decreased from 458.86 m/s to 332.14 m/s at the exit whereas angular velocity *(U)* was 500.12 m/s and 518.30 m/s at the inlet and exit, respectively. Contrary to rotor blades, stator blades decrease the C and A increases at the exit of the stator blade. CFD analysis of the first stage rotor blades was shown in Fig. 6. Relative velocity *(W)* decreased at the inlet from 346 m/s to 262 m/s at the exit with flow separation at the inlet of the blades (see Fig. 6(a)). The total enthalpy of the air was around 668 kj/kg and did not change significantly at the rotor blades (see Fig. 6(b)). The total temperature and a pressure change of the flow showed the constant average temperature, which was determined to be 635 K that was increased with the total pressure from inlet to exit. The maximum pressure was detected to be 1815 kPa where this pressure was observed left pressure side of the rotor blades at the flow with the average Mach number of 1.09 (see Fig.6(c), (d) and (e)). Stress analysis results in Fig. 6(f) showed that the maximum stress observed near the blade roots with 462 MPa at the first stage of the rotor.

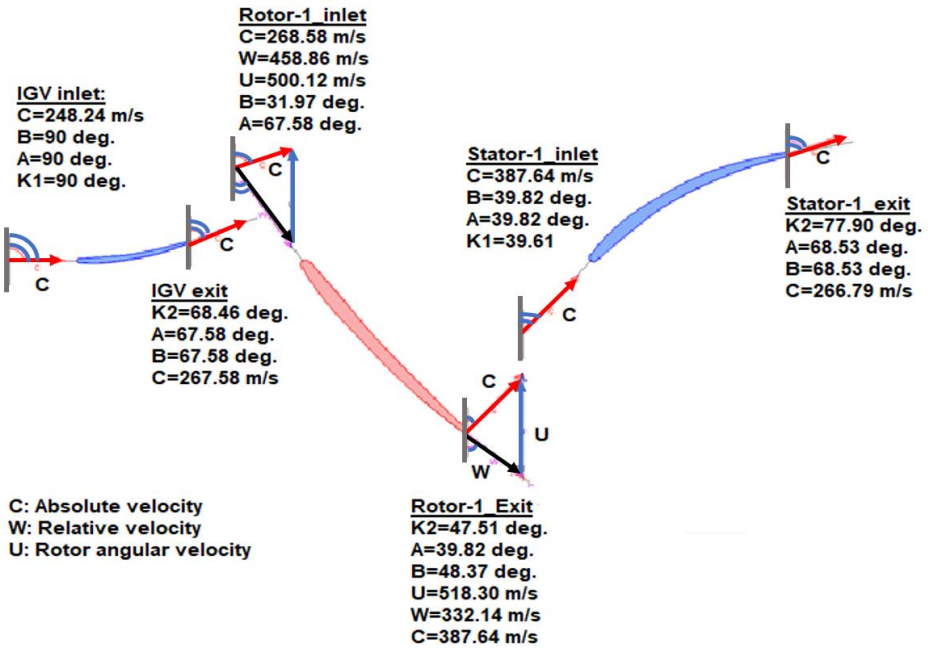

Figure 5. Velocity vectors of the first stage with rotor and stator inlet and exit analysis.

When looking at the velocity calculation results of the stator blades, inlet C was 387.64 m/s and angles were determined to be K1=39.61° whereas A and B were 39.82° (see Fig. 5). This velocity and angles changed to C=266.78 m/s, K=68.53°, B=68.53°, A=77.90° at the exit of the stator blades. Stator blades decreased the absolute velocity to the inlet of rotor blades at the exit that provided almost constant absolute velocity at the stage. Thermodynamics and stress analysis of the stator blades are shown in Fig. 7. The relative velocity of the flow decreased from 440 m/s to 272 m/s which was close to *C* exit value at the rotor (see Fig. 7(a)). The average total pressure and the temperatures were 942 kPa and 616 K at the stator blades exit, respectively (see Fig. 7(b), (d)). The total enthalpy changed from 578.7 kj/kg to 607.2 kJ/kg at the stator related to absolute velocity decrease at the inlet and exit of the stator (see Eq. 1 and Fig. 7(c)).

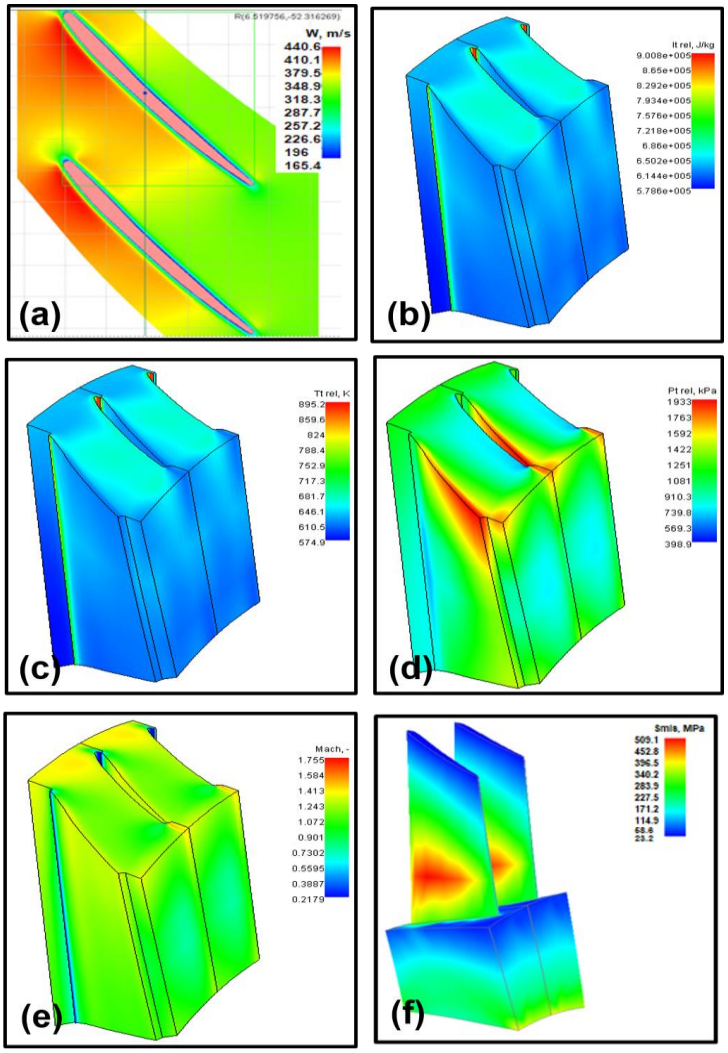

Figure 6. First stage rotor thermodynamic and stress analysis, (a) relative velocity of the flow, (b) total enthalpy change of the flow, (c) total temperature change, (d) total pressure change, (e), Mach analysis, (f) stress analysis of the blades.

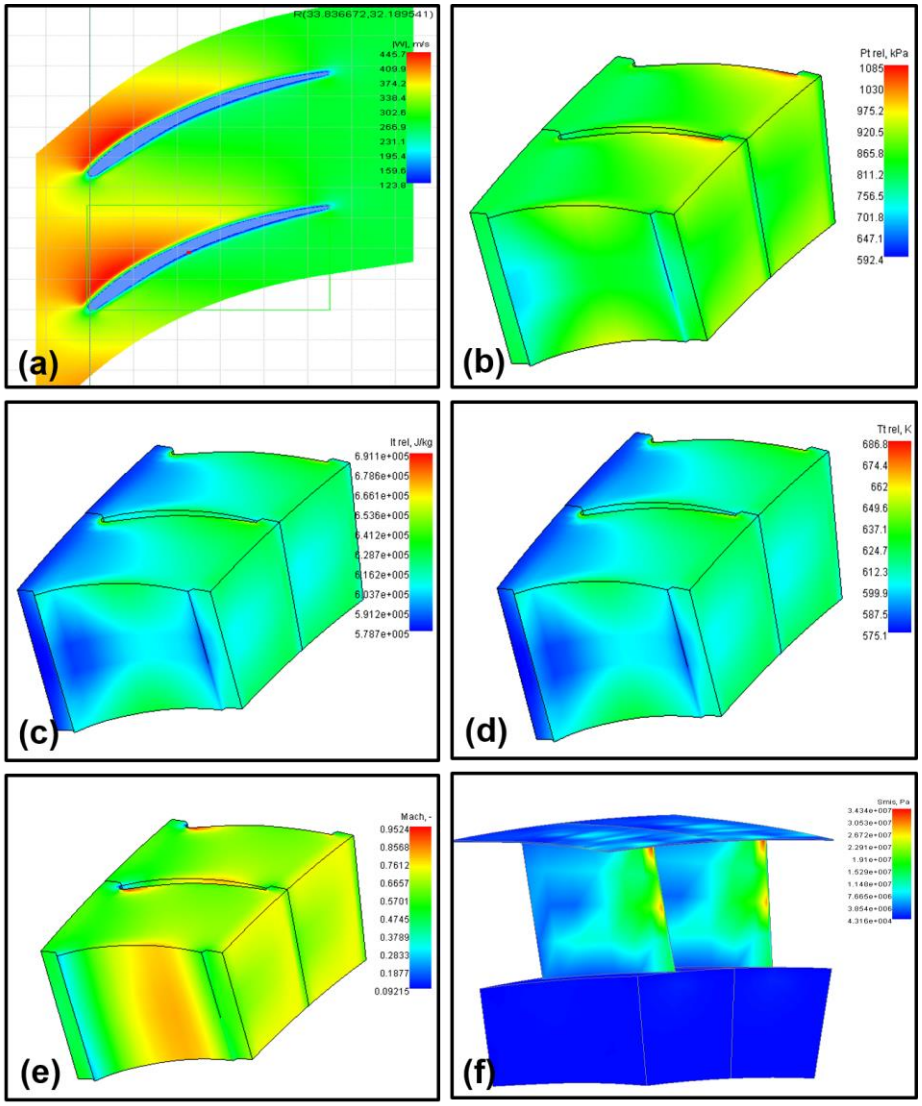

Figure 7. First stage stator thermodynamic and stress analysis, (a) relative velocity of the flow, (b) total enthalpy change of the flow, (c) total temperature change, (d) total pressure change, (e), Mach analysis, (f) stress analysis of the blades.

Stator bladed decreased significantly the Mach number which decreased from 1.09 to 0.74 at the exit of stator blades (see Fig. 7(e)). The stress was high at the exit sides of the blades with 30.5 MPa which is very low when compared to rotor blades (see Fig. 7(f)).

3.2.3. Fifth Stage Analysis

Fig. 8 shows the velocity diagram of the last stage consisted of the rotor and stator blades of the axial compressor. The inlet and exit absolute velocity of the stage was 265 m/s. Therefore, the absolute velocity of the air at the combustion chambers was 265 m/s. K1 and K2 were changed from 23.22° to 49.93°, 41.81° to 81.45° at the inlet and exit of the last stage. CFD analysis of the last stage of the axial compressor is shown in Fig. 9. According to the results, the relative velocity of the air (546 m/s) at the inlet of the stage dropped to 264.38 m/s at the exit. Furthermore, the total pressure of the air at stage exit was found to be 2651 kPa which was close to the design criteria of 2643 kPa (see Fig. 9 (c) and (d)). The total temperature changed from 932 K to 857 K with the total enthalpy change from 942 to 857 kj/kg at the inlet and exit of the stage that shows total inlet temperature and enthalpy of the air at the inlet of combustion chambers (see Fig. 9 (e) and (f)).

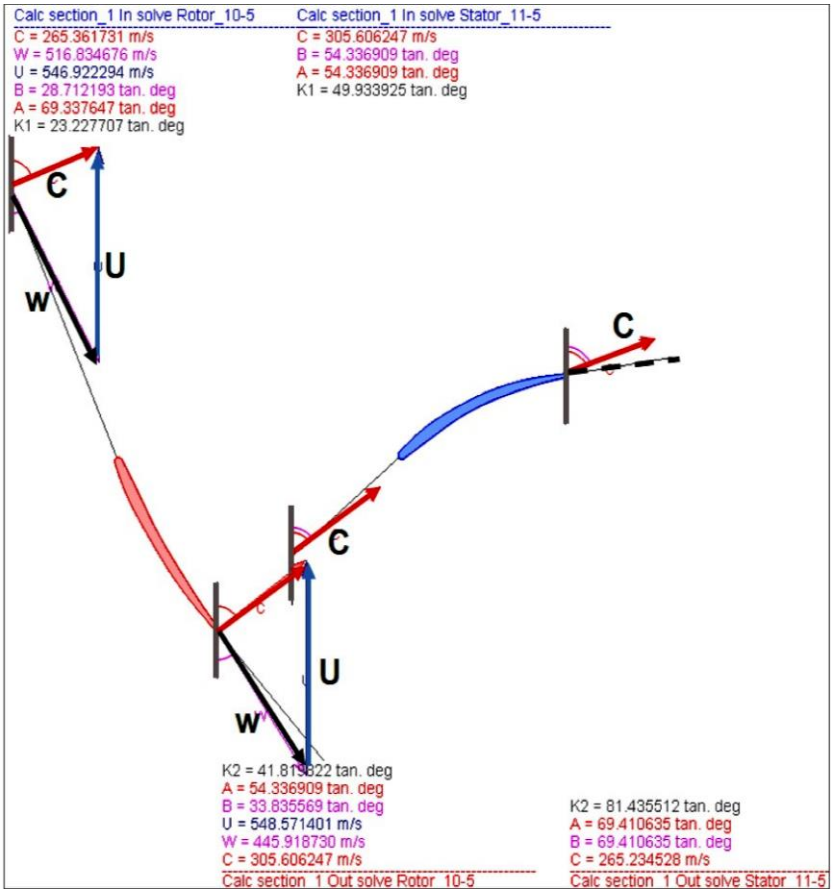

Figure 8. Velocity diagram of the last stage of the axial compressor.

The Mach number decreased from 0.95 to 0.49 at the exit of the stage (see Fig. 10 (c) and (d)). The maximum stress of the rotor blades was 365 MPa whereas this stress was determined to be 82 MPa for stator blades (see Fig. 10 (a) and (b)).

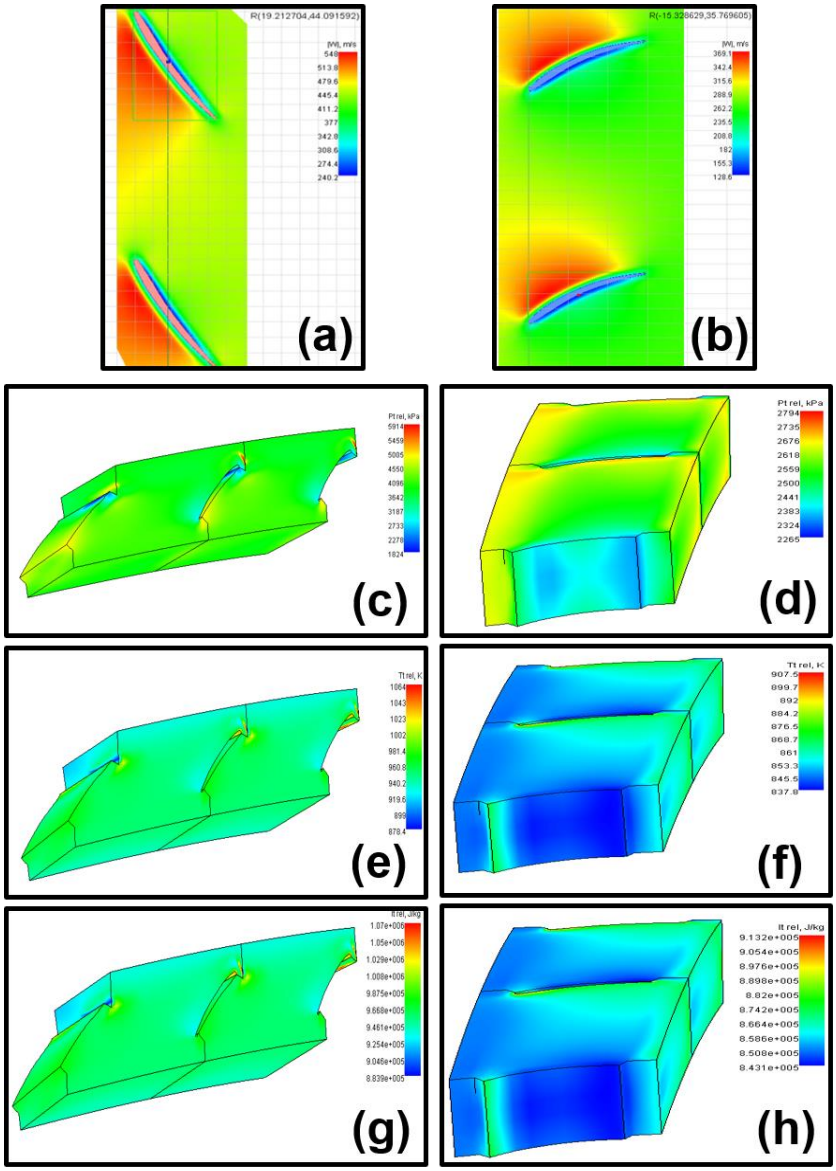

Figure 9. Flow analysis of the last stage, (a), (b) relative velocity of the flow at rotor and stator blades, (c), (d) total temperature change of the flow, (e), (f) total temperature change, (g), (h) total enthalpy change of the flow at rotor and stator blades.

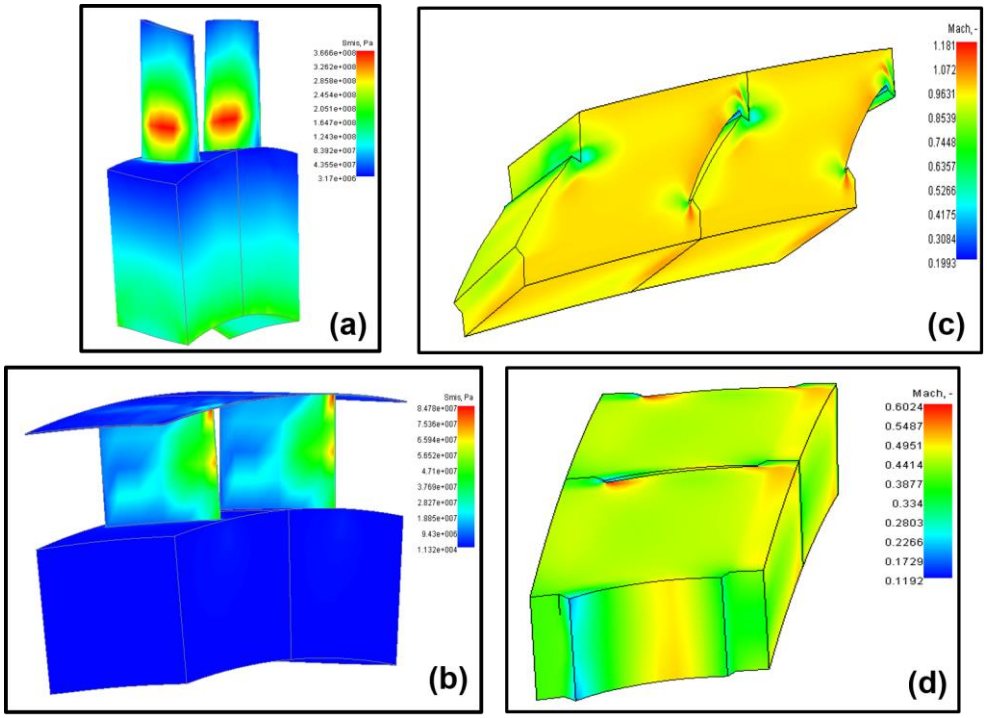

Figure 10. (a), (b) stress analysis of the rotor and stator blades, (c), (d) Mach number analysis of the flow at rotor and stator blades.

4. DISCUSSION

In this study, an axial compressor consisted of 5 stages was designed and analyzed by using AxStream software for a turbofan engine. The design of the compressor was compared to an actual turbofan engine compressor which is used in military aviation. Our design exit temperature at IGV was 487 K which was closed to the actual IVG exit temperature of 475 K. Meanwhile, the last stage temperature was found to be 857 K and this also similar to the actual compressor exit temperature of 833 K. On the other hand, the calculated exit pressure of the designed compressor was 2651 kPa whereas actual compressor pressure was determined to be 2643 kPa.

The results showed that exit temperatures and pressures of the designed compressor were 97% close to the actual compressor. The calculated polyprotic efficiency of the designed compressor was 90% which is higher than reported actual compressor efficiency of 88 %. Nickel-chromium alloy X UNS 06002 was selected as compressor blade material consisted of 8.5 Mo, 21 Cr, 18 Fe, 0.6 W (% in weight). The maximum working temperature and tensile stress of the material blade are 1200 °C and 572.74 MPa. The calculated maximum stress of first and the last stage rotor blades were 462, 365 MPa which are in the safe working limits. On the other hand, the compressor exit temperature of 857 K was lower than the maximum temperature of the blade material. The contribution of the rotor to the increase in pressure is expressed by the reaction rate by rate of rotor and stator pressure differences. Here, the calculated reaction rate was 0.47 close to 50 % that set out the symmetric stage means static pressure increase in stage formed by an equivalent contribution of the rotor and stator. Furthermore, aimed pressure can be achieved with a lower stage by using the symmetric stage and it minimizes the surge and stall in the compressor [15].

5. CONCLUSION

An axial compressor was designed and analyzed with AxStream software for a turbofan engine which is used in military aviation. Five stages of axial compressor velocity, thermodynamics, stress, and CFD analysis were performed. According to this basic analysis, the following conclusion can be drawn:

- Although, rotor blades increased the absolute velocity at the exit stator blades decreased absolute velocity to the inlet of the rotor at the stage. This shows that pressure increase was evaluated at constant absolute velocity.
- CFD analysis of the airflow in the designed compressor showed similar pressure, temperature, and total efficiency with an actual compressor.
- The polyprotic efficiency of the designed compressor was 2 % higher than the actual compressor.
- AxStream is a powerful software for design and analysis of gas turbines main components such as axial compressor, fan, and turbine.

REFERENCES

[1] Bathie, W.W., (1996). Fundamentals Of Gas Turbines, Second Edition, John Wiley&Sons Inc., Canada.

[2] Eyüp, Ö., (1997). Türbin Motorlarının Aerotermodinamiği ve Mekaniği Esaslar ve Uygulamalar, Birsen Yayın Evi, İstanbul.

[3] Fletcher, P. Philip, W.P., (2004). Gaz Turbine Performance, Second Edition, Blackwell Publishing company, Malden, MA, USA.

[4] Giampaolo, T., (2006). Gas Turbine Handbook: Principles and Practices, Third Edition, The Fairmont Press., USA.

[5] Arthur, G.J., (1994). Turbine Design and Application, NASA Scientific and Technical Informantion Program, Washington D.C., USA.

[6] Rama, G.S.R., Aijaz, K.A., (2003). Turbomachinery Design and Theory, Marcel Dekker Inc., USA.

[7] Theodero, G., (2001). Compressor Performance: Aerodynamics For The User, Second Edition, Elsevier Science & Technology Books, U.S.A.

[8] Dorfner, C., Hergt, A., Nicke, E., & Moenig, R. (2011). Advanced Nonaxisymmetric Endwall Contouring for Axial Compressors by Generating an Aerodynamic Separator—Part I: Principal Cascade Design and Compressor Application. Journal of Turbomachinery, 133(2), 021026.

[9] Richard, H.T.C., (1981). Gas Turbine Engineering Applications, Cycles and Characteristics, The Macmillan Press LTD., London/United Kingdom.

[10] Horlock J.H. (2003). Advanced Gas Turbine Cycles, Elsevier Science LTD., Oxford, United Kingdom.

[11] Samad, A., Kim, K.-Y. (2008). Shape optimization of an axial compressor blade by multi-objective genetic algorithm. Proceedings of the Institution of Mechanical Engineers, Part A: Journal of Power and Energy, 222(6), 599–611.

[12] Yamada, K., Furukawa, M., Nakakido, S., Matsuoka, A., & Nakayama, K. (2015). Large-Scale DES Analysis of Unsteady Flow Field in a Multi-Stage Axial Flow Compressor at Off-Design Condition Using K Computer. Volume 2C: Turbomachinery.

[13] Moroz, L., Govorushchenko, Y., Pagur, P. (2006). A Uniform Approach to Conceptual Design of Axial Turbine / Compressor Flow Path, 3rd International Conference, The Future of Gas Turbine Technology, 1-11.

[14] Boyce, M.P., (2006). Gas Turbine Engineering Handbook, Third Edition, Oxford, UK.

[15] Ikeguchi, T., Matsuoka, A., Sakai, Y., Sakano, Y., & Yoshiura, K. (2012). Design and Development of a 14-Stage Axial Compressor for Industrial Gas Turbine. Volume 8: Turbomachinery, Parts A, B, and C.

Journal of Naval Sciences and Engineering
2020, Vol. 16, No.1, pp.25-44
Physics/Fizik

RESEARCH ARTICLE

ANNEALING TEMPERATURE EFFECTS ON SURFACE MORPHOLOGY AND OPTICAL PROPERTIES OF IGZO THIN FILMS PRODUCED BY THERMAL EVAPORATION

Atılgan ALTINKÖK[1]
Murat OLUTAŞ[2]

[1]*National Defense University, Turkish Naval Academy, Electrical and Electronics Engineering, Istanbul, Turkey,*
aaltinkok@dho.edu.tr; ORCID: 0000-0002-0548-4361

[2]*Bolu Abant Izzet Baysal University, Faculty of Arts and Sciences, Physics Department, Bolu, Turkey,*
olutas_m@ibu.edu.tr; ORCID: 0000-0002-6250-6977

Date of Receive: 06.03.2020 **Date of Acceptance: 31.03.2020**

ABSTRACT

The use of Transparent Conductive Oxide (TCO) thin films in technology has increased in the last decades. These materials have good electrical conductivity visible light transmittance simultaneously. TCOs have many technology applications such as thin film transducers (TFTs), conductive electrodes, capacitors, sensors, electrochemical devices. Although indium tin oxide (ITO) is the most common semiconductor among these materials, studies on N-type indium-gallium-zinc oxide (IGZO) that better electrical properties (electron mobility μFE>10 cm^2 /V.s) cm^2 / Vs) have increased in recent years. In this study, IGZO thin films are produced which have a very homogeneous amorphous structure via using thermal evaporation system on glass substrates. Structural characterization was carried out by atomic force microscopy and scanning electron microscopy on IGZO thin films for various thickness and annealing temperatures. Transmittance and thickness measurements were performed using UV-VIS spectroscopy and profilometer

for the investigation of optical properties, respectively. It is seen that grain size grows and grain boundaries decreases when annealing temperature is increased. This results in reduced roughness and increased optical transmittance and energy gap (Eg).

Keywords: *IGZO, AFM, Thin Film, Band Energy.*

Annealing Temperature Effects on Surface Morphology and Optical Properties of IGZO Thin Films Produced by Thermal Evaporation

TAVLAMA SICAKLIĞININ TERMAL BUHARLAŞTIRMA İLE ÜRETİLEN IGZO İNCE FİLMLERDE YÜZEY MORFOLOJİSİ VE OPTİK ÖZELLİKLERE ETKİSİ

ÖZ

Saydam İletken Oksit (TCO) ince filmlerin teknolojide kullanımı son yıllarda artmıştır. Bu malzemeler aynı anda iyi bir elektrik iletkenliğine ve görünür ışık geçirgenliğine sahiptir. TCO'lar, ince film dönüştürücüler (TFT'ler), iletken elektrotlar, kapasitörler, sensörler, elektrokimyasal cihazlar gibi birçok teknoloji uygulamasında kullanılmaktadırlar. İndiyum kalay oksit (ITO) bu malzemeler arasında en yaygın kullanılan malzeme olmasına rağmen, daha iyi elektriksel özelliklere (elektron hareketliliği μFE>10 cm^2 /V.s) cm^2 / Vs) sahip olan N tipi indiyum-galyum-çinko oksit (IGZO) üzerinde yapılan çalışmalar günümüzde önem kazanmıştır. Bu çalışmada, cam alttaş üzerinde termal buharlaştırma sistemi kullanılarak yüksek vakum altında oda sıcaklığında çok homojen bir amorf yapıya sahip IGZO ince filmler üretilmiştir. Üretilen IGZO ince filmlerin yapısal karakterizasyonu ise Atomik kuvvet mikroskobu ve taramalı elektron mikroskobu kullanılarak çeşitli kalınlık ve tavlama sıcaklıkları için gerçekleştirilmiştir. Geçirgenlik ve kalınlık ölçümleri ise optik özelliklerin araştırılması için sırasıyla UV-VIS spektroskopisi ve profilometre kullanılarak yapılmıştır. Tavlama sıcaklığı arttıkça tanecik boyutunun büyüdüğü ve tane sınırlarının azaldığı görülmektedir. Bu durum, pürüzlülüğün azalmasına ve optik geçirgenliğin ve enerji boşluğunun (E_g) artmasına neden olmaktadır.

Anahtar Kelimeler: *IGZO, AFM, İnce Film, Band Enerjisi.*

1. INTRODUCTION

Transparent Conductive Oxides (TCO's) are materials that have good optical permeability and good electrical conductivity generally. They are mostly composed of special double or triple compounds and contain at least one metallic element. A good TCO has an optical transparency of around 80%, an energy band range of over 3 eV and a low resistivity value of 10-3 Ω.m. These properties can be improved by improving oxygen or by doping different metals to the pure TCO samples. Thus, we can obtain materials with a better optical transparency and electrical properties. As a sample of TCO, Zinc oxide (ZnO) thin films have high optical permeability, electrical conductivity, magnetic - piezo electricity and wide energy band gap (~ 3.4 eV) within this framework. These superior features allow ZnO thin films to be used in the areas of the LCDs, solar cells, thin film transistors and chemical gas sensors [1-8]. ZnO thin films can be produced by different methods such as magnetron sputter, spray pyrolysis and thermal evaporation, [9-15]. Studies on ZnO have shown an increase in the 1990's and its importance has increased with the presence of technological applications nowadays. Metal oxide materials, such as ZnO, have a wide band range of semiconductors in the II-VI semiconductor group, so they do not have sufficient electrical conductivity for technological applications alone. In order to maintain high optical permeability and to create materials with lower resistivity, it is necessary to create correct stoichiometric composition or doping.

Recently, researchers have made metal contributions to ZnO in order to improve electrical conductivity and optical permeability for the further development of technology applications of ZnO thin films. Aluminum-ZnO (AZO), Gallium-ZnO (GZO), Indium-ZnO (IZO) and Indium-Gallium-ZnO (IGZO) thin films are produced in this way. The most important reason for choosing materials such as indium, aluminum and gallium is that the Ionic diameters of these metals are close to the ion diameters of the zinc. Thus, Zn atoms can be replaced within the lattice matrix.

Although doping indium or gallium separately to the ZnO has investigated in the literature, the properties of doping of these two metals together to ZnO are still in the under the research. These type of materials are called

InGaZnO (IGZO). IGZO is a special material that attracts the most attention among the oxide semiconductor materials and also has semiconductor material properties [16-20]. Furthermore, there are technological application possibilities such as high electron mobility (> 10 cm^2 / V.s), reproducibility at room temperature and low temperature devices. Today, IGZO studies have begun to be published and are often focused on the device characteristics and atomic ratio and [19, 21-23]. In addition, in many articles, there are studies related to the annealing temperature of IGZO thin films [24].

In the technological applications of IGZO thin films, there are difficulties in the resistance of films and interfacial problems [22, 24-26].] In order to use these in technology more effectively, detailed investigation of the effects of preparation conditions such as chemical composition (dependence of the doping ratios) and annealing temperature on the samples is needed. One of the world's biggest technology company Sharp is produced crystal oxide semiconductor screen and they have started to use the first IGZO application on the screens in recent years. Smartphones, tablets and touch screens produced within the scope of these products have received awards from many parts of the world [27].

In this study, IGZO films were deposited on Si/SiO and glass substrates via thermal evaporation method [28] at various annealing temperatures. The effect of annealing temperatures on the structural, optical physical and opto-electrical properties of IGZO films was investigated.

2. MATERIALS AND METHOD

Semiconducting IGZO film samples were grown on Si/SiO and glass substrates by a thermal evaporation (Vaksis MİDASm PVD/2T) operating at a base pressure of 5 x 10^{-5} mbar. The typical deposition rates were kept constant at 0.5 nm/s for the samples. The IGZO thin films were prepared onto glass substrates using indium (In), gallium (Ga) and zinc (Zn) metals with the weight ratio of 1:1:1 wt% (In:Ga:Zn). In order to evaporate of metals, a tungsten boat was used for every metal. The glass substrates were cleaned by acetone, distilled water and ultrasonic cleaner. To prepare the IGZO thin film, the indium metal was firstly deposited, then gallium metal was deposited and finally zinc metal was deposited onto glass substrate under 10^{-5} mbar pressure. Five IGZO thin film samples were annealed for thermal oxidation at different temperatures for 1 hour in the program controller muffle furnace (Nabertherm L5 S27). One of the thin film called as deposited (IGZO-AD) which is without annealing, other four thin films were annealed at different temperatures, 475, 500, 550 and 600 °C. The samples were called according to their annealing temperatures as IGZO-475, IGZO-500, IGZO-550 and IGZO-600. profilometer.

Thickness of the thin film samples was checked with a KLA Tencor P6 profilometer. Thickness of IGZO thin films was around 221 nm IGZO-AD, 169 nm, 152 nm, and 149 nm and 134 nm as the annealing temperature of IGZO thin films was 475, 500, 550 and 600 °C, respectively.

Surface nanostructures of IGZO samples were investigated by scanning electron microscope (Hitachi- SU1510). In order to investigate morphological properties of IGZO samples, atomic force microscopy (Nanosurf Flex-5) was used. These AFM images were obtained in the non-contact mode [29, 30]. [29, 30]. The scan was performed on the field of 25 μm with 1 line per second at a resonance frequency of about 160 kHz. Several fields were scanned on the sample surfaces. The optical properties of the ITO thin film samples were studied on the basis of transmittance and absorbance measurements, and these measurements in wavelength range from 300 to 1000 nm was carried out by a Shimadzu UV Mini-1240 Uv-Vis

spectrophotometer. The optical band gap energy values and porosity of the films are calculated by this the transmittance spectra.

3. RESULTS AND DISCUSSION

Figure 1 (a) - (e) shows SEM images of the IGZO-AD, IGZO-475, IGZO-500, IGZO-550 and IGZO-600 thin films, respectively. Surfaces of the samples seem to be formed by grains and the grains have different shapes and sizes. The porous structures can also be seen from SEM images. After annealing, it was seen that the surface roughness decreases and the grains are larger in Figure 1 (b) and (c). Thanks to the annealing process, thin film samples have not only gained a transparent appearance, but have also shown a lower resistance and become more homogeneous due to the effect of oxygen. In Figure 1 (d), the grain sizes on the surface of the sample with an annealing temperature of 550 ^{o}C start to shrink again and become smaller. As the temperature increases, a more dense grained structure is formed. In Figure 2 (e), due to the high annealing temperature value, the particle structure on the surface of the sample has disappeared and a transition has started from amorphous structure to crystal structure [31]. Also, at this temperature, the transparency of the film was significantly reduced and its resistance increased significantly. The best transparency of the thin film samples was obtained at annealing temperature at 475 ° C.

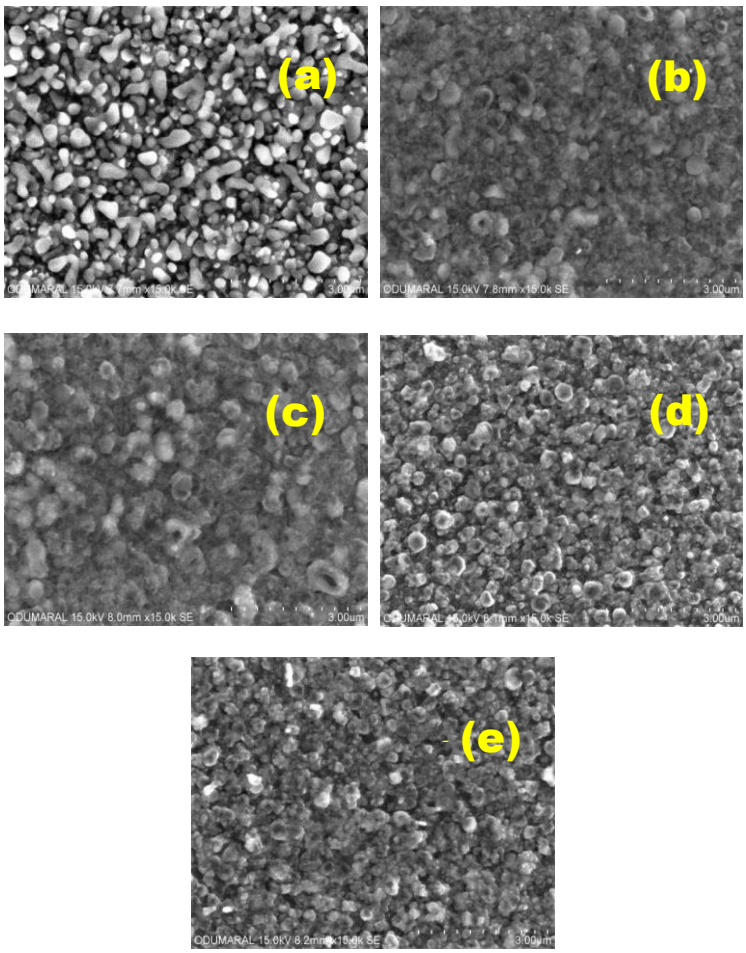

Figure 1. SEM images of (a) IGZO-AD; (b) IGZO-475; (c) IGZO-500; (d) IGZO-550; (e) IGZO-600.

AFM images of the surfaces of thin films produced at different annealing temperatures are shown in figure 2 (a) - (e).The AFM roughness results are summarized in Table 1. As seen from the table 1 , the IGZO-475 sample has the lowest surface, roughness as 32.964 nm among the films while IGZO-AD found to be the highest roughness values, without annealing, as 74.713 nm. In addition to this, the different surface roughness values can be interpreted as the lack of the oxygen [32, 33].

Table 1. Summary of AFM roughness results.

Sample	Average roughness (Sa) (nm)	RMS roughness (Sq) (nm)
IGZO-AD	74.713	92.781
IGZO-475	32.964	46.013
IGZO-500	59.503	97.182
IGZO-550	42.221	61.269
IGZO-600	68.754	85.05

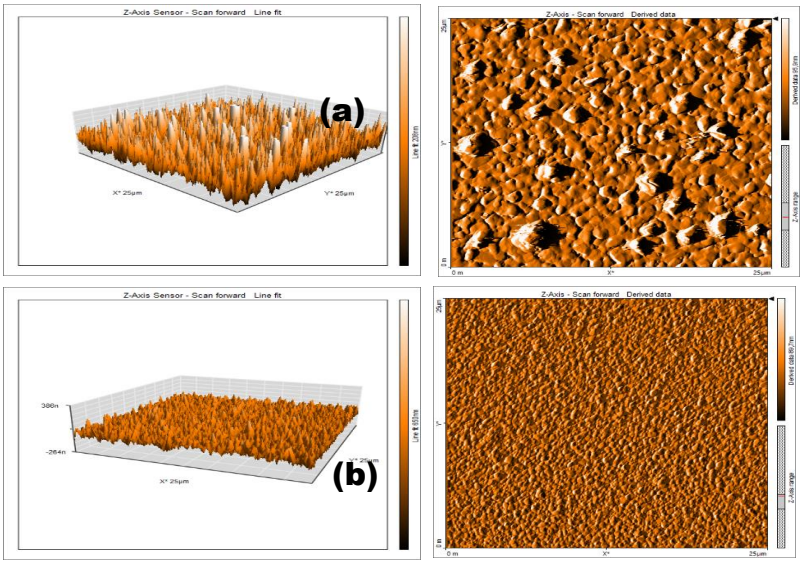

Figure 2. Atomic force microscopy (AFM) images of the IGZO films annealed at (a) as deposited; (b) 475 °C;

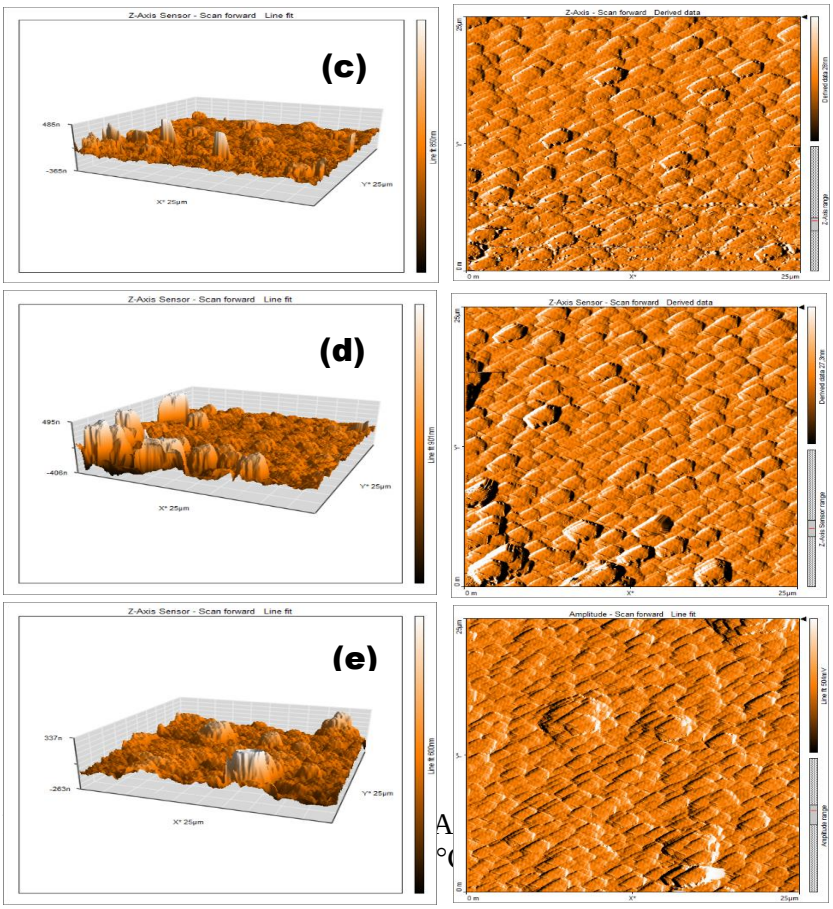

Figure 2. Atomic force microscopy (AFM) images of the IGZO films annealed at (c) 500 °C; (d) 550°C; and (e) 600 °C.

Figure 3 shows the transmittance spectra of the IGZO films as a function of wavelength in the range of 300 to 900 nm. The average transmittance ratio of IGZO thin films was 14%, 33%, 27 %, 28.5 % and 25 %, respectively. The decrease in the optical transmittance value is due to the formation of oxygen vacancies [34, 35] and large grains [36], which is supported by AFM results.

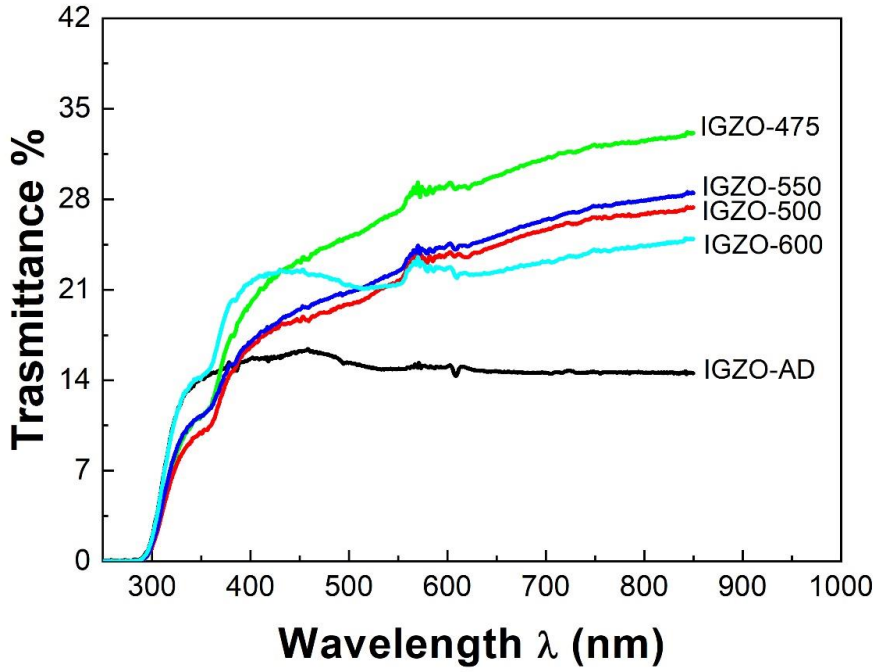

Figure 3. Optical transmittance spectra in visible region of the IGZO Samples.

There are several methods to calculate optical band gap energy (Eg) of the materials in the literature. In this study, to determine the energy gap of the samples the absorption coefficient α of the thin films were evaluated using

the optical transmittance spectra and the absorption coefficient was calculated using Equation (1) [36]

$$\alpha = \frac{\left[\ln\left(\frac{1}{T}\right)\right]}{d} \qquad (1)$$

where T is transmittance, d is the film thickness. In addition, the dependence of the absorption coefficient on the incident photon energy is given by [38]

$$(\alpha h\nu) = B(h\nu - E_g)^{1/2} \qquad (2)$$

where B characteristic parameter, E_g denotes the energy bandgap, $h\nu$ is the photon energy. Thus extrapolation of the straight-line portion of the plot of $(\alpha h\gamma)^2$ versus photon energy $(h\nu)$ to zero absorption (α=0) gives the direct band gap of the films.

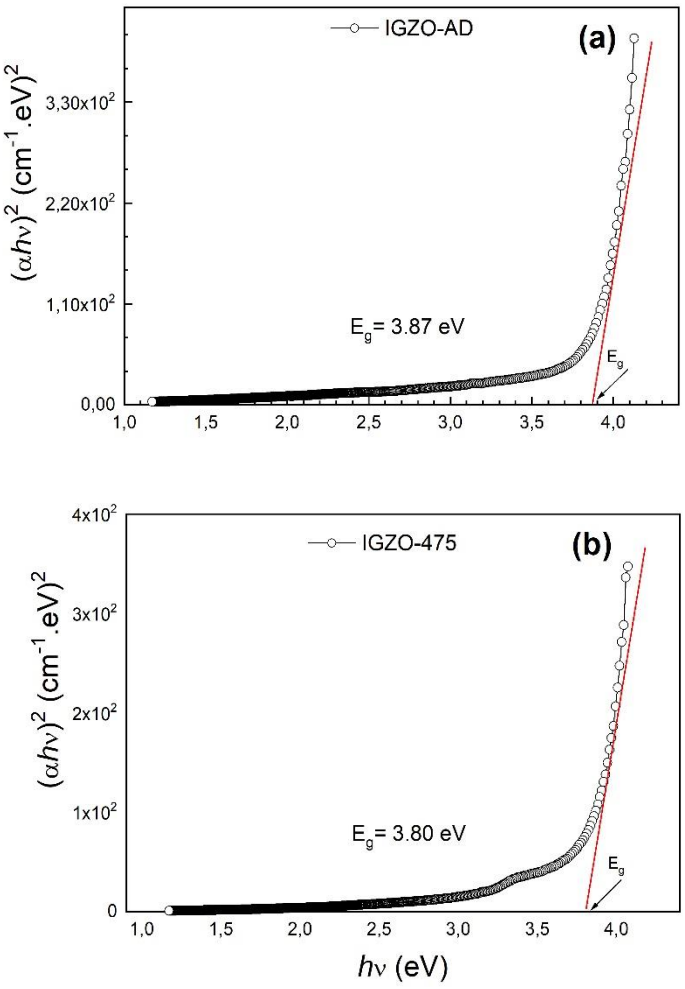

Figure 4. Variation of the optical band gap of IGZO thin films: (a) as deposited (without annealing); (b) 475˚C.

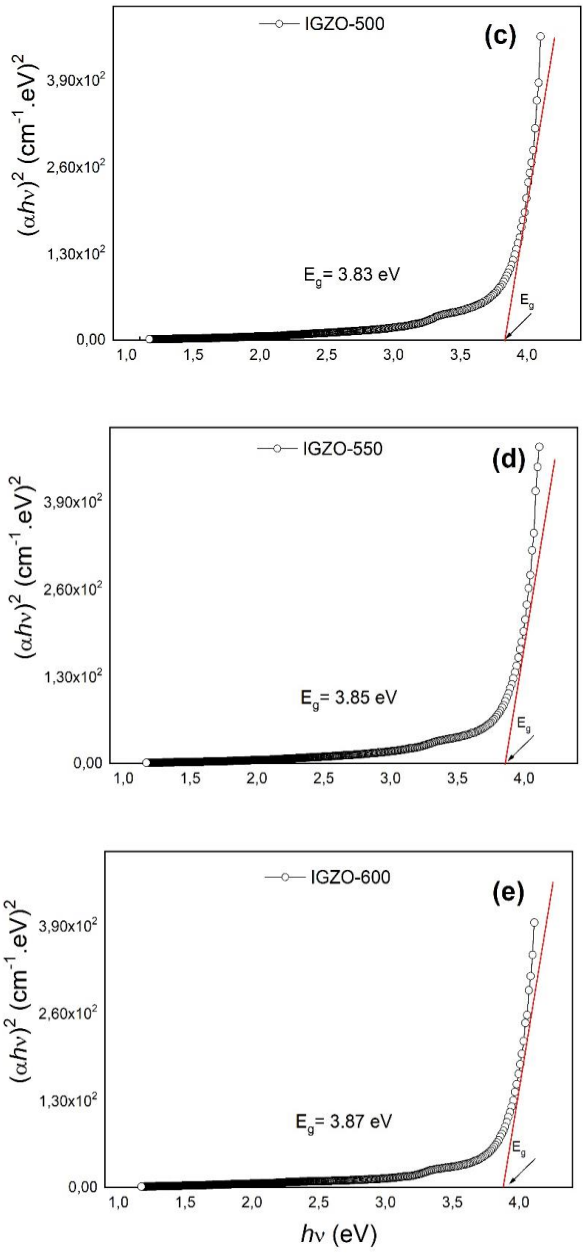

Figure 4. Variation of the optical band gap of IGZO thin films: (c) 500; (d) 550˚C and (e) 600˚C.

Figure 4 (a)-(e) shows the calculated values of the band gap energies (E_g) of IGZO thin films were 3.87 eV, 3.80 eV, 3.83 eV, 3.85 eV and 3.87 eV as the annealing temperatures were As-deposited, 475, 500, 550 and 600 °C, respectively. While increasing the annealing temperature the bandgap energy decreases then it reaches its previous value with the increase of annealing temperatures further.

Generally, higher band gap value causes low optical absorption. Observing low absorption in the visible range is a main characteristic of metal oxide semiconductors (MOS), having a band gap energy of above 3 eV.

4. CONCLUSION

In this study, polycrystalline IGZO thin films were deposited on glass and Si/SiO substrates by thermal evaporation technique at room temperature. it is investigated that how the annealing temperature affects the microstructural and optical properties of the IGZO thin films. Characterization of the samples was conducted by atomic force microscopy, scanning electron microscopy, UV-VIS spectroscopy. The results showed that Structural, optical, morphological properties of the thin films are strongly dependent on annealing temperature. The grain size is increased by temperature. Without annealing sample (IGZO-AD) has the highest Average roughness (74.713 nm) while IGZO-475 has the smallest roughness 32.964 nm. The maximum transmittance is observed to be 33 % for the IGZO-475 sample while the minimum transmittance is observed to be 14 % for the IGZO-AD film as a result of the different grain sizes and roughness. While the maximum energy gap has the 3.87 eV for the IGZO-600 sample the minimum band gap energy value is 3.80 eV for IZGO-475 sample. This is of the opinion that it is related to the structural disorder existing at the grain boundaries.

5. ACKNOWLEDGEMENTS

This work was supported by Giresun University Research Fund under project number FEN-BAP-A-230218-26.

REFERENCES

[1] Zhang, M. L., Jin, F., Zheng, M. L., Liu, J., Zhao, Z. S., & Duan, X. M. (2014). High efficiency solar cell based on ZnO nanowire array prepared by different growth methods, Rsc Advances, 4(21), pp. 10462-10466.

[2] Choi, Y. S., Kang, J. W., Hwang, D. K., & Park, S. J. (2009). Recent advances in ZnO-based light-emitting diodes, IEEE Transactions on electron devices, 57(1), pp. 26-41.

[3] T. P. H. Sidiropoulos, R. Roder, S. Geburt, O. Hess, S. A. Maier, C. Ronning, and R. F. Oulton, (2014). Ultrafast plasmonic nanowire lasers near the surface plasmon frequency, Nat Phys, 10, p. 870.

[4] Yun, D. J., & Rhee, S. W. (2009). Deposition of Al-doped ZnO thin-films with radio frequency magnetron sputtering for a source/drain electrode for pentacene thin-film transistor, Thin Solid Films, 517(16), pp. 4644-4649.

[5] Kumar, R., Al-Dossary, O., Kumar, G., & Umar, A. (2015). Zinc oxide nanostructures for NO 2 gas–sensor applications: A review, Nano-Micro Letters, 7(2), pp. 97-120.

[6] Cai, A., Du, L., Wang, Q., Chang, Y., Wang, X., & Guo, X. (2016). Kelp-inspired N–I-doped ZnO photocatalysts with highly efficient catalytic activity, Materials Science in Semiconductor Processing, 43, pp. 25-33.

[7] Cao, X., Li, X., Gao, X., Liu, X., Yang, C., Yang, R., & Jin, P. (2011). All-ZnO-based transparent resistance random access memory device fully fabricated at room temperature, Journal of Physics D: Applied Physics, 44(25), p. 255104.

[8] Struk, P., Pustelny, T., Gut, K., Golaszewska, K., Kaminska, E., Ekielski, M., & Piotrowska, A. (2009). Planar optical waveguides based on thin ZnO layers. Acta Physica Polonica-Series A General Physics, 116(3), p. 414.

[9] Jayaraman, V. K., Kuwabara, Y. M., & Álvarez, A. M. (2016). Importance of substrate rotation speed on the growth of homogeneous ZnO thin films by reactive sputtering, Materials Letters, 169, pp. 1-4.

[10] Tsoutsouva, M. G., Panagopoulos, C. N., Papadimitriou, D., Fasaki, I., & Kompitsas, M. (2011). ZnO thin films prepared by pulsed laser deposition, Materials Science and Engineering: B, 176(6), pp. 480-483.

[11] Hasim, S. N. F., Hamid, M. A. A., Shamsudin, R., & Jalar, A. (2009). Synthesis and characterization of ZnO thin films by thermal evaporation, Journal of Physics and Chemistry of Solids, 70(12), pp. 1501-1504.

[12] Duan, L., Zhao, X., Zhang, Y., Shen, H., & Liu, R. (2016). Fabrication of flexible Al-doped ZnO films via sol–gel method, Materials Letters, 162, pp. 199-202.

[13] Ergin, B., Ketenci, E., & Atay, F. (2009). Characterization of ZnO films obtained by ultrasonic spray pyrolysis technique, International journal of hydrogen energy, 34(12), pp. 5249-5254.

[14] Ali, M. M. (2011). Characterization of ZnO thin films grown by chemical bath deposition, Journal of Basrah Researches (Sciences), 37(3A), pp. 49-56.

[15] Huang, Y., Sarkar, D. K., & Chen, X. G. (2015). Superhydrophobic nanostructured ZnO thin films on aluminum alloy substrates by electrophoretic deposition process, Applied Surface Science, 327, pp. 327-334.

[16] Nomura, K., Ohta, H., Takagi, A., Kamiya, T., Hirano, M., & Hosono, H. (2004). Room-temperature fabrication of transparent flexible thin-film transistors using amorphous oxide semiconductors, nature, 432(7016), pp. 488-492.

[17] Leppänen, K., Saarela, J., Myllylä, R., & Fabritius, T. (2013). Electrical heating synchronized with IR imaging to determine thin film defects, Optics express, 21(26), pp. 32358-32370.

[18] Kim, S., Jeon, Y. W., Kim, Y., Kong, D., Jung, H. K., Bae, M. K., & Park, J. (2011). Impact of oxygen flow rate on the instability under positive bias stresses in DC-sputtered amorphous InGaZnO thin-film transistors, IEEE Electron Device Letters, 33(1), pp. 62-64.

[19] Kikuchi, Y., Nomura, K., Yanagi, H., Kamiya, T., Hirano, M., & Hosono, H. (2010). Device characteristics improvement of a-In–Ga–Zn–O TFTs by low-temperature annealing, Thin Solid Films, 518(11), pp. 3017-3021.

[20] Matsuo, T., Mori, S., Ban, A., & Imaya, A. (2014, June). 8.3: Invited paper: advantages of IGZO oxide semiconductor, In SID Symposium Digest of Technical Papers (Vol. 45, No. 1, pp. 83-86).

[21] Nakata, M., Takechi, K., Eguchi, T., Tokumitsu, E., Yamaguchi, H., & Kaneko, S. (2009). Flexible high-performance amorphous InGaZnO4 thin-film transistors utilizing excimer laser annealing, Japanese Journal of Applied Physics, 48(8R), 081607.

[22] Gosain, D. P., & Tanaka, T. (2009). Instability of amorphous indium gallium zinc oxide thin film transistors under light illumination, Japanese Journal of Applied Physics, 48(3S2), 03B018.

[23] Ohara, H., Sasaki, T., Noda, K., Ito, S., Sasaki, M., Endo, Y.,& Yamazaki, S. (2010). 4.0-inch active-matrix organic light-emitting diode display integrated with driver circuits using amorphous In–Ga–Zn-Oxide thin-film transistors with suppressed variation, Japanese Journal of Applied Physics, 49(3S), 03CD02.

[24] Godo, H., Kawae, D., Yoshitomi, S., Sasaki, T., Ito, S., Ohara, H., & Yamazaki, S. (2010). Temperature dependence of transistor characteristics and electronic structure for amorphous In–Ga–Zn-Oxide thin film transistor, Japanese Journal of Applied Physics, 49(3S), 03CB04.

[25] Takechi, K., Nakata, M., Eguchi, T., Yamaguchi, H., & Kaneko, S. (2009). Temperature-dependent transfer characteristics of amorphous InGaZnO4 thin-film transistors, Japanese Journal of Applied Physics, 48(1R), 011301.

[26] Takechi, K., Nakata, M., Eguchi, T., Yamaguchi, H., & Kaneko, S. (2009). Comparison of ultraviolet photo-field effects between hydrogenated amorphous silicon and amorphous InGaZnO4 thin-film transistors, Japanese Journal of Applied Physics, 48(1R), 010203.

[27] M. o. E. chunichi Industry and Technology Award (27th), Trade and Industry Award.

[28] Durdu, S., Aktug, S. L., Aktas, S., Yalcin, E., Cavusoglu, K., Altinkok, A., & Usta, M. (2017). Characterization and in vitro properties of anti-bacterial Ag-based bioceramic coatings formed on zirconium by micro arc oxidation and thermal evaporation, Surface and Coatings Technology, 331, pp. 107-115.

[29] Tsarkova, L., Knoll, A., Krausch, G., & Magerle, R. (2006). Substrate-induced phase transitions in thin films of cylinder-forming diblock copolymer melts, Macromolecules, 39(10), pp. 3608-3615.

[30] Zalakain, I., Ramos, J. A., Fernandez, R., Etxeberria, H., & Mondragon, I. (2012). Silicon and carbon substrates induced arrangement changes in poly (styrene‐b‐isoprene‐b‐styrene) block copolymer thin films, Journal of applied polymer science, 125(2), pp. 1552-1558.

[31] De Meux, A. D. J., Pourtois, G., Genoe, J., & Heremans, P. (2015). Comparison of the electronic structure of amorphous versus crystalline indium gallium zinc oxide semiconductor: structure, tail states and strain effects, Journal of Physics D: Applied Physics, 48(43), 435104.

[32] Ling, L., Tao, X., Zhongxiao, S., Chunliang, L., & Fei, M. (2016). Effect of sputteringpressure on surface roughness, oxygen vacancy and electrical properties of a-IGZO thin films, Rare Metal Materials and Engineering, 45(8), pp. 1992-1996.

[33] de Jamblinne de Meux, A., Bhoolokam, A., Pourtois, G., Genoe, J., & Heremans, P. (2017). Oxygen vacancies effects in a‐IGZO: Formation mechanisms, hysteresis, and negative bias stress effects, physica status solidi (a), 214(6), 1600889.

[34] Li, X., Wang, Y., Liu, W., Jiang, G., & Zhu, C. (2012). Study of oxygen vacancies′ influence on the lattice parameter in ZnO thin film, Materials Letters, 85, pp. 25-28.

[35] Liu, H., Zeng, F., Lin, Y., Wang, G., & Pan, F. (2013). Correlation of oxygen vacancy variations to band gap changes in epitaxial ZnO thin films, Applied Physics Letters, 102(18), 181908.

[36] Ahmed, N. M., Sabah, F. A., Abdulgafour, H. I., Alsadig, A., Sulieman, A., & Alkhoaryef, M. (2019). The effect of post annealing temperature on grain size of indium-tin-oxide for optical and electrical properties improvement, Results in Physics, 13, 102159.

[37] Valencia, S., Marín, J. M., & Restrepo, G. (2009). Study of the bandgap of synthesized titanium dioxide nanoparticules using the sol-gel method and a hydrothermal treatment, The Open Materials Science Journal, 4(1).

[38] J.N. Hodgson, Optical Absorption and Dispersion in Solids, Chapman & Hall, London, 1970.

Journal of Naval Sciences and Engineering
2020, Vol. 16, No.1, pp.45-70
Mechanical Engineering/Makine Mühendisliği

RESEARCH ARTICLE

EFFECT OF THE NITRIDING PROCESS IN THE WEAR BEHAVIOUR OF DIN 1.2344 HOT WORK STEEL

Seda ATAŞ BAKDEMİR[1]
Doğuş ÖZKAN [2]
M. Cenk TÜRKÜZ [3]
Elif UZUN[4]
Serdar SALMAN[5]

[1]*National Defence University, Turkish Naval Academy, Mechanical Engineering Department, Istanbul, Turkey, sabakdemir@dho.edu.tr; ORCID: 0000-0003-1601-2033*

[2]*National Defence University, Turkish Naval Academy, Mechanical Engineering Department, Istanbul, Turkey, dozkan@dho.edu.tr; ORCID: 0000-0002-3044-4310*

[3]*Titanit Ultra Hard PVD Coatings Company, Istanbul, Turkey, cenk.turkuz@titanit.com.tr; ORCID: 0000-0002-4447-7287*

[4]*Marmara University, Metallurgical and Materials Engineering Department, Istanbul, Turkey, elif.uzun@marmara.edu.tr; ORCID: 0000-0002-4950-2162*

[5]*National Defence University, Rectorate of National Defense University, Istanbul, Turkey, ssalman@marmara.edu.tr; ORCID: 0000-0002-9184-3876*

Date of Receive: 08.03.2020 **Date of Acceptance: 02.04.2020**

Seda ATAŞ BAKDEMİR, Doğuş ÖZKAN, M. Cenk TÜRKÜZ, Elif UZUN, Serdar SALMAN

ABSTRACT

Gas nitriding is a widely applied thermochemical surface treatment, which is applied to enhance mechanical properties and wear characteristics of iron and steels. The impact of the gas nitriding process on the mechanical and wear resistance characteristic of DIN 1.2344 (X40CrMoV5-1) hot work steel were investigated in this paper. Nitrided and non-nitrided samples were characterized through a different method such as the optical microscope, scanning electron microscopy, energy dispersive spectrometry, X-ray diffraction, atomic force microscope (AFM) and 3D optical profilometer. The results of analyses reveal that increases in wear resistance of the nitrided sample due to the formation of surface layers of nitrides and oxides.

Keywords: *Gas Nitriding, Wear Behavior, DIN 1.2344 Steel, Atomic Force Microscope.*

Seda ATAŞ BAKDEMİR, Doğuş ÖZKAN, M. Cenk TÜRKÜZ, Elif UZUN, Serdar SALMAN

NİTRASYON İŞLEMİNİN DIN 1.2344 SICAK İŞ TAKIM ÇELİĞİNİN AŞINMA DAVRANIŞLARI ÜZERİNE ETKİLERİ

ÖZ

Gaz nitrasyon yöntemi demir ve çeliklerin mekaniksel özelliklerini ve aşınma karakteristiklerini geliştirmek için uygulanan bir termokimyasal yüzey işlemidir. Bu çalışmada DIN 1.2344 (X40CrMoV5-1) sıcak iş takım çeliğine uygulanan gaz nitrasyon işleminin mekanik özelliklerine ve aşınma direncine etkisi araştırılmıştır. Nitrürlenmiş numune ve işlem görmemiş referans numune optik mikroskop, SEM EDX, X ışını difraksiyonu, atomik kuvvet mikroskopu ve 3D optik profilometre yoluyla karakterize edilmiştir. Analiz sonuçları nitrürlenmiş numune yüzeyinde oluşan nitrür alaşımları ve oksidasyon tabakası sayesinde aşınma direnci artış meydana geldiğini göstermiştir.

Anahtar Kelimeler: *Gaz Nitrasyon, Aşınma Davranışı, DIN 1.2344 Çeliği, Atomik Kuvvet Mikroskopu.*

1. INTRODUCTION

The success of high technology countries is mostly the result of continuous and efficient running systems in industrial applications. The effective life of system components is an important phenomenon in mechanical systems [1]. In recent years, there has been a growing submission for surface treatments that can alter the surface properties of different materials by developing their physical and chemical characteristics like wear and corrosion resistance, hardness, fatigue strength, coefficient of friction, etc [2]. The nitriding is a famous process for supplying surfaces with better tribological properties [3]. The nitriding process is a thermochemical surface treatment based on the development of the surface with nitride phases in consequence of the diffusion of nitrogen ions into the material surface [4]. The nitriding process is carried out at low temperature as compared with alternative surface hardening techniques such as carburizing and carbonitriding. Hereby the steel stays in the ferrite phase (or cementite depending on the alloy composition) along the process. Quenching is not needed in the nitriding process and thanks to distortions are at the minimum level. Additionally, the nitriding process is comparatively practical to audit by process parameters and core hardness [5].

The formation of the nitrided case results from the “compound layer” and “diffusion zone" from the surface to the core. Two different structures are shown in Figure 1. The field under the diffusion zone is the core of the steel including tempered martensite. The compound layer contains epsilon phase (ε -$Fe_{2-3}N$), gamma phase (γ-Fe_4N) or a mixed-phase ($\varepsilon+\gamma$) [6]. Phase structure and thickness of the compound layer notably influence the material's mechanical properties. A longer nitriding time is needed to form γ-Fe_4N whereas ε -$Fe_{2-3}N$ can easily be formed on the surface and grown over time because the γ-Fe_4N structure that can nucleated and grown within the ε structure [7]. The fact that the white layer consists only of these intermetallic compounds ensures that the hardness is independent of the chemical composition of the material. However, the white layer has an extremely hard and fragile structure. Therefore, it can cause material deformation and crack under contact conditions [8]. Meanwhile, the white

layer should be reduced or removed greatly by some methods such as grinding and chemical dissolution from the surface before using the nitrided part. The nitrogen is found as an intermediary atom in the iron cubic or finely dispersed alloy nitride in the diffusion zone. The hardness value decreases due to the decreasing amount of nitrogen in the inner parts of the steel [9]. While the white layer contributes to the development of the corrosive properties, the diffusion layer improves the tribological properties and fatigue strength of the steels [10].

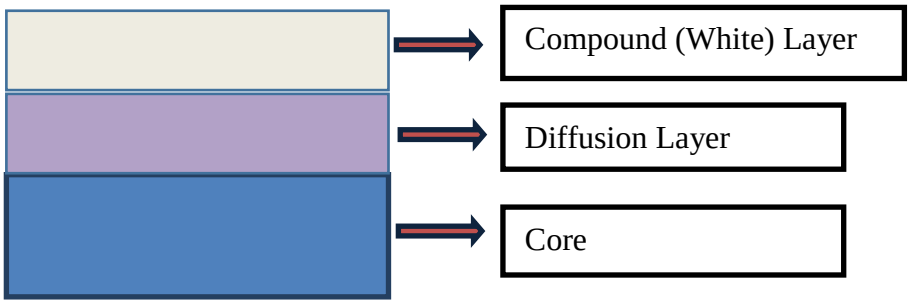

Figure 1. Formation nitrided case [6].

There are three types of nitriding methods: gas, liquid and ion nitriding which Ammonia is used in gas nitriding. Nitrogen decomposes from ammonia gas, reacts with iron and alloy elements in steel and then forms fine-grained nitrides. Liquid nitriding is done in salt baths containing NaCN. Some of the nitrogen and carbon in the cyanide (CN) penetrate the steel. Ion nitriding is based on the ionization and bombardment of a mixture of gases such as nitrogen and hydrogen, on the surface of the material [11].

DIN 1.2344 is widely used in hot die applications, die casting and extrusion dies, wear-resistant tools, high pressure die casting tools and pressing tools. Since DIN 1.2344 hot work steel is exposed to a compeller mechanical and thermal shocks, its wear and corrosion resistance, hardness should be improved through several surface treatments [12]. This study presents the wear and friction behavior of gas nitrided DIN 1.2344 hot work steel. Previous works showed that the wear rate belongs to the thickness of the

nitrided layer and hardness, toughness [13]. Wear and friction tests were carried out at three different contact pressures. The effect of plasma nitriding discussed in the light of wear rates of the nitrided sample and bare steel comparison with wear mechanisms evaluation.

Table 1. Chemical composition of the DIN 1.2344 hot work steel [14].

Element	**C**	**Si**	**Cr**	**Mo**	**V**
Wt %	0,40	1,00	5,30	1,40	1,00

2. MATERIALS AND METHODS

2.1. Substrate Preparation

DIN 1.2344 (X40CrMoV5-1) hot work steel substrates (30x30x5mm) were selected as the base material. The chemical composition of DIN 1.2344 hot work steel is shown in Table 1 [14]. Before nitriding processes, the substrate should be subjected to some pretreatments for sufficient hardness [15]. The samples are heat-treated by using the consequent steps: austenitizing at 1030°C for 25 minutes, quenching, and after all double tempering (at 590°C and 600°C for 2 hours to remove the internal stresses in the steel. After the first tempering, the expected impact of rough carbide which has a brittle structure, occurred by the transformation of austenite to tempered martensite is reduced during the second tempering step [16]. Substrates were polished to Rq=19.98 nm quadratic surface roughness (measured with atomic force microscopy (AFM)) with sandpapers and then cleaned with isopropanol for 15 min. by the ultrasonic cleaner.

2.2. Nitriding Process and Characterization

Treatments were realized in a gas nitriding furnace which was preheated to 450 °C where the ambient air consists of ammonia and nitrogen gas mixture. The temperature was set to 530˚C during the active nitriding process [17]. The nitrided samples were grinded and polished after mounting with bakelite mold metallographic examination. Polished samples were etched

for about 10-15 seconds with 5% Nital [18]. The thickness and microstructures of nitrided layers were observed by an optical microscope. Average (Ra), root mean square roughness (Rq) of the nitrided sample and bare steel sample were obtained by AFM (Nanosurf Flex AFM-5) topography analysis. Surface structure and chemical composition of the nitrided sample and bare steel sample were investigated via SEM Zeiss Ultra Plus field emission scanning electron microscope) and EDX (Bruker XFlash 5010 EDX detector with 123 eV resolution). To specify the phases in the nitrided specimens, X-ray diffractometry (XRD) by the use of Bruker D8 Advance X-ray diffractometer was performed.

2.3. Tribometer Test Condition and Test Parameters

Tribometer (UTS 10/20) with a ball on the flat reciprocating module device was operated to determine the wear behavior of the samples and to obtain the friction coefficient values.

Table 2. Tribometer test condition and test parameters.

Load [N]	5/10/15
Frequency [Hz]	2
Stroke [mm]	5
Sliding Distance [m]	100
Temperature [°C]	24 °C

Alumina balls with a diameter of 6 mm are used at wear test. According to the parameters given in Table 2, wear tests of nitrided and bare steel samples were performed at 5, 10, and 15N loads.

The maximum Hertzian contact pressure was assessed by eq.(1) (: load, $\mathbf{E'}$: Effective elastic modulus, : diameter of the ball) [19].

$$P_{maks} = \frac{1}{\pi}\left(\frac{6xLxE'^2}{R^2}\right)^{\frac{1}{3}} \quad (1)$$

The observed maximum Hertzian contact pressure of the nitrided sample and bare steel sample were shown in Table 3.

Table 3. Hertzian contact pressure.

	Hertzian Contact Pressure (GPa)	
	DIN 1.2344 Bare Steel	**DIN 1.2344 Nitriding**
5N	1.28	1.35
10N	1.61	1.70
15N	1.84	1.95

2.4. Surface and Tribochemical Analysis

Morphological changes and wear mechanisms formations were observed by optical microscope and AFM analysis. Wear scar surfaces were scanned via force modulation mode by using uncoated silicon nitride (Si_3N_4) rectangular PPP-LFMR cantilever with the spring constant of 0.178 N/m. The surface energy of the samples was carried out force-distance mapping on the surfaces with a 16x16 force curve analysis with SPIP 6.7.8 analysis. Wear volumes of the wear scars were evaluated with scanning of the all wear scar surface by an optical profilometer (Sensofar) and then raw data examined with Mountainspip 8 software. Tribochemical evaluation of the tribofilms and worn surfaces were carried out SEM/EDX.

3. RESULTS AND DISCUSSION

3.1. Characterization of The Nitriding Process

X-ray diffraction pattern of this sample showed that the nitriding layer included mainly of α-Fe that slightly γ and ε nitrides formed after the nitriding process (see Figure 2)[6]. A thin compound layer was detected above the diffusion zone that can be explained by the XRD phase analysis diagram which is similar in both samples. This layer is the brittle white layer formed by iron nitrides and it can be removed from the surface by abrasive methods after nitriding [20].

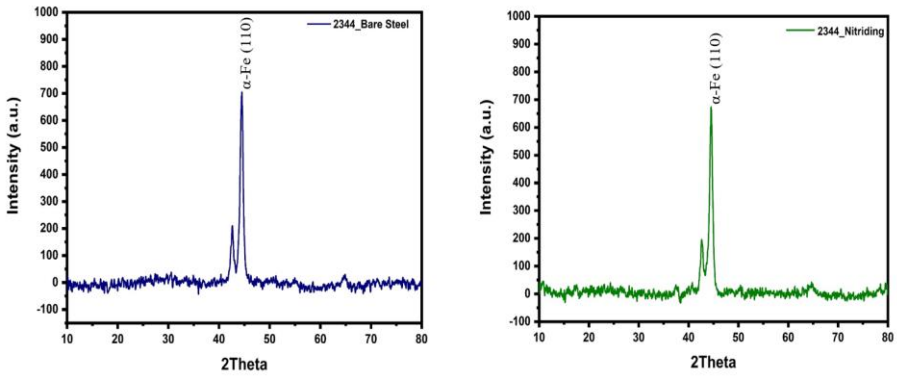

Figure 2. XRD patterns of the 2344 bare steel and 2344 nitrided steel.

The optical microscope, AFM and SEM/EDX images of the samples are shown in Figure 3. AFM topography analysis showed that bare steel and nitrided steel had a different average surface roughness (Ra) and root mean square roughness (Rq), 15.32, 6.64 and 19.98, 8.67 nm, respectively. The decrease in the roughness values of the nitrided surface improved the wear properties. SEM/EDX images showed the nitrogen phase compatibly XRD analysis results. Nitrogen was detected on the nitriding sample surface

where the decrease in iron amount indicates the formation of iron nitride structures [21].

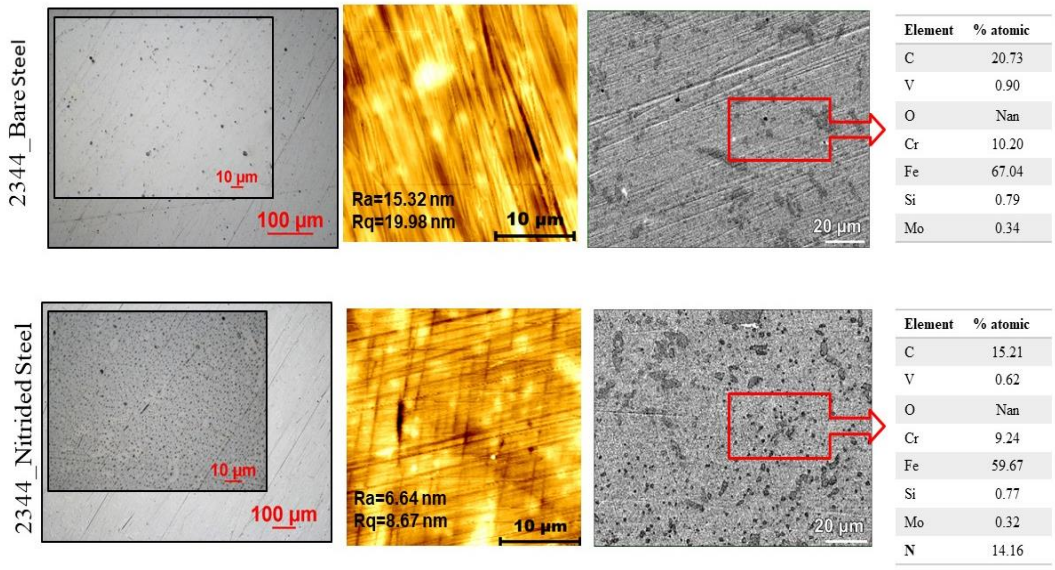

Element	% atomic
C	20.73
V	0.90
O	Nan
Cr	10.20
Fe	67.04
Si	0.79
Mo	0.34

Element	% atomic
C	15.21
V	0.62
O	Nan
Cr	9.24
Fe	59.67
Si	0.77
Mo	0.32
N	14.16

Figure 3. Optical microscope, AFM and SEM/EDX images of the bare steel and nitrided sample.

3.2. Friction Coefficients and Wear Rates

Friction coefficients results are shown in Figure 4. Wear tests are applied at three different loads, the sample that was nitrided under all loading conditions showed a lower friction coefficient. The COFs of 2344 bare steel sample was found to be 1.13, 0.96, 1.15 at 5, 10, 15N, whereas 2344 nitrided steel COFs were 0.58, 0.52, 0.95 at 5, 10, 15N, respectively. The friction coefficient values of 2344 nitrided steel at the 5 and 10 N was approximately 55% lower than the 2344 bare steel. On the other hand, similar COFs were observed at 15N [22]. In addition, the nitriding layer broke down at the sliding distance of 40 m where the COF increase started at 15N.

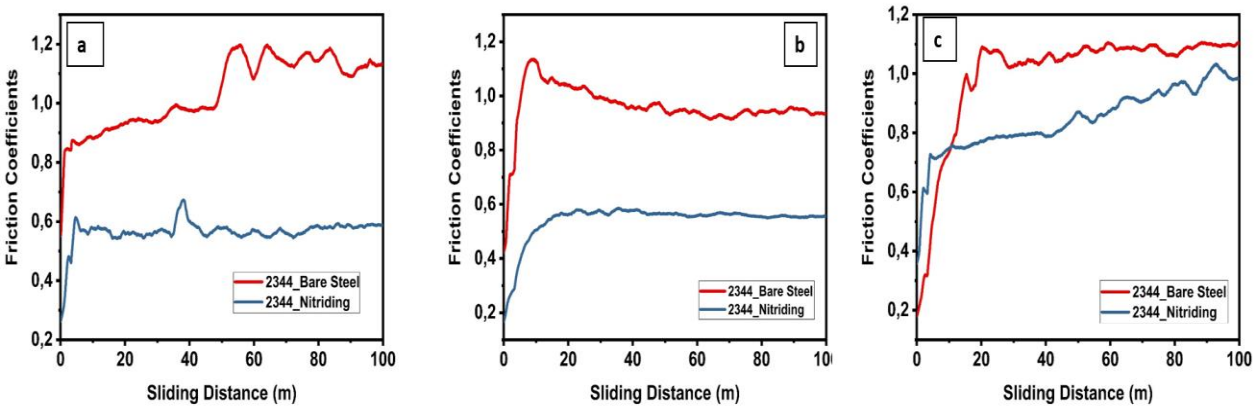

Figure 4. Friction coefficient evaluations (a) COFs at 5 N, (b) COFs at 10 N, (c) COFs at 15 N.

Rockwell C hardness measurement was performed on the sample surfaces under 150 kgf load as shown in Figure 5. The brittle structure on the top of the nitride layer caused cracks in the hardness trace.

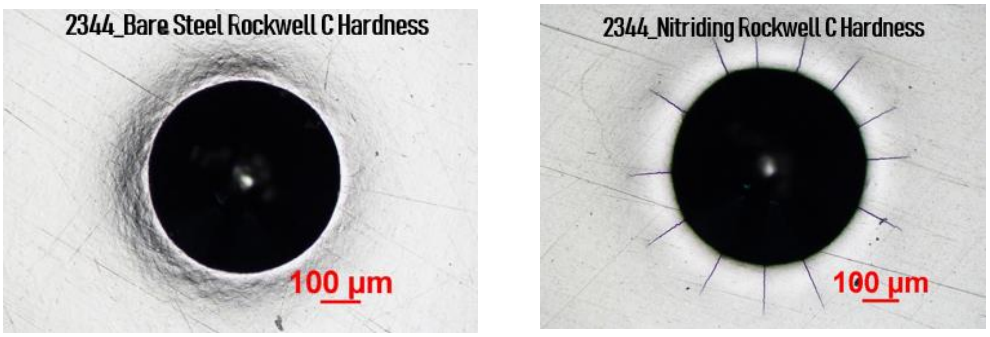

Figure 5. Rockwell C hardness scar of 2344 bare steel and 2344 nitrided steel at 150kgf.

The thickness and microstructures of nitrided and layers were shown in Figure 6. The thickness of the total nitrided layer was measured as 77.99 µm [23].

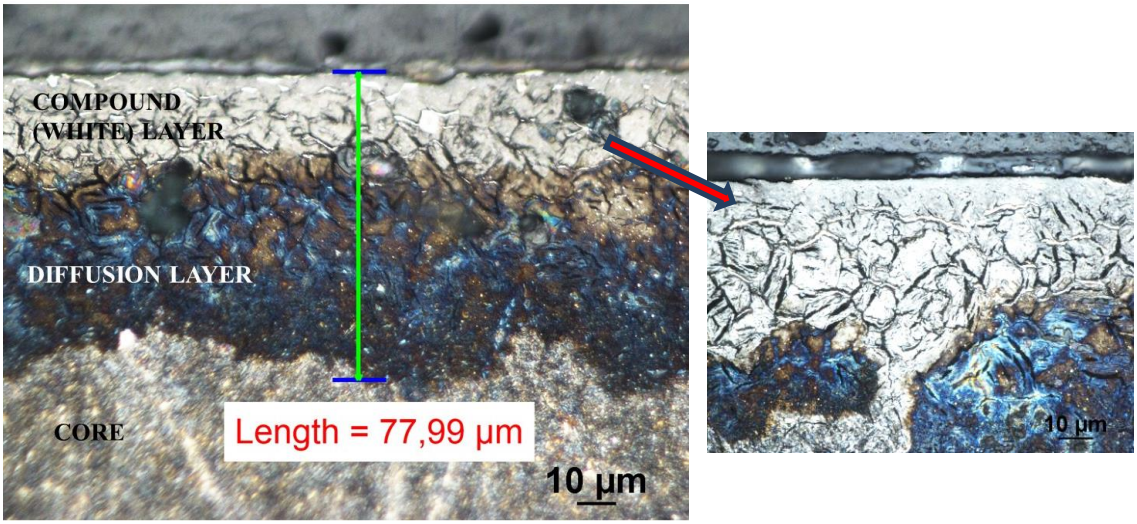

Figure 6. Optical microscope image of the formation nitrided case.

After wear tests, wear line widths of the samples and counter surface images of the alumina ball were obtained with an optical microscope (see Figure 7). The 2344 bare steel sample wear widths were measured to be 425.65, 693.27, 719.72 µm at 5, 10, 15N, respectively and the abrasive wear lines wear homogeneously formed throughout all scars. Wear widths increased with load at the same time, on the other hand, the amount of wear transfer element originated from the counter surface alumina increased with the load. Therefore, the worn area diameter of the alumina ball increases with load. When compared to the wear scar widths of samples, the nitrided sample had approximately 60% lower wear scar width against the bare sample. Abrasive wear lines are not dominant at 5 and 10N, but abrasive wear lines were observed as labeled with yellow arrows at 15N load. The higher wear transfer material was observed on the alumina ball as a result of the high contact pressure at 15N.

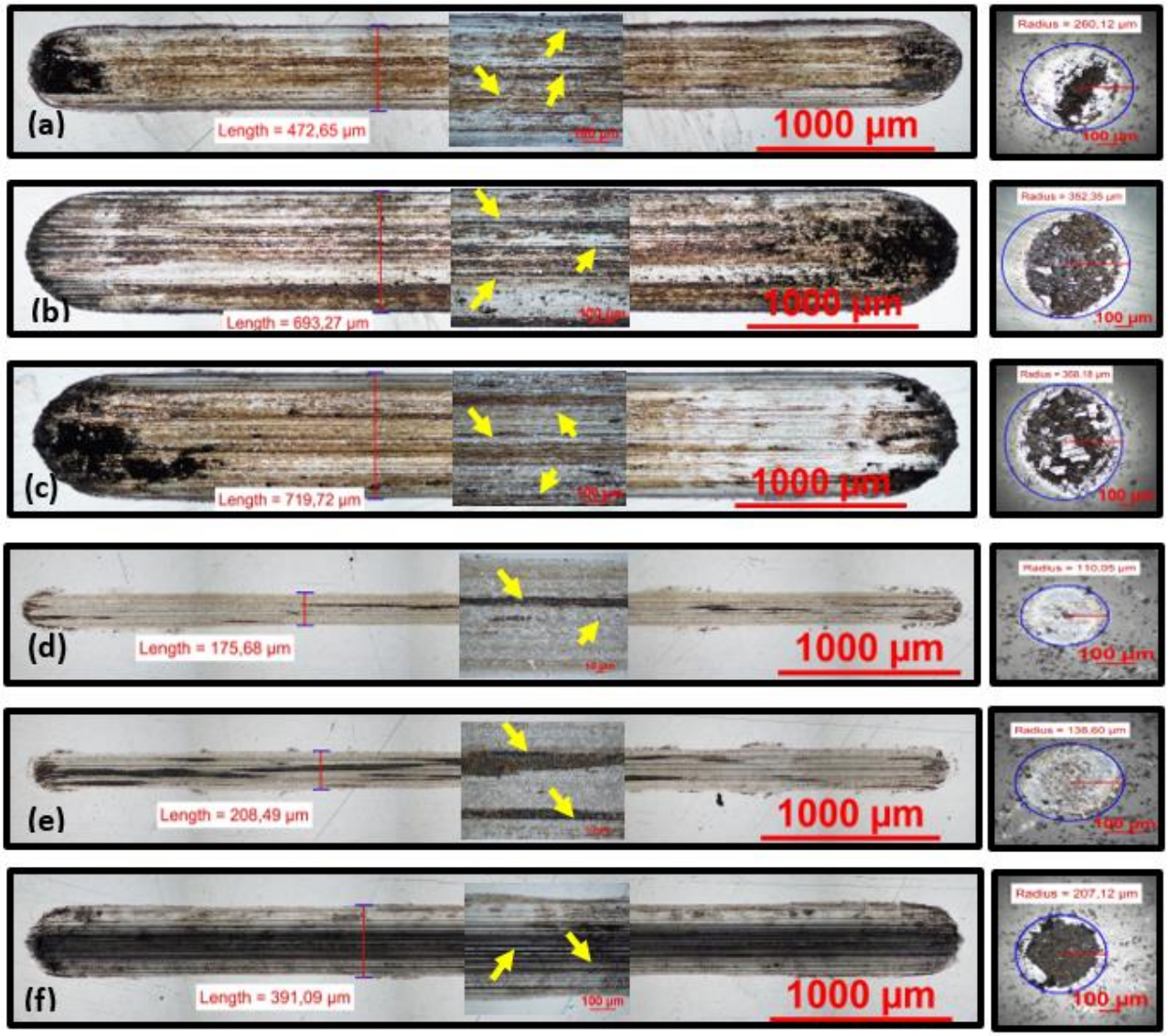

Figure 7. Optical microscope images of the wear scars and alumina ball surfaces, (a), (b), (c) 2344 Bare steel and ball tested at 5,10 and 15N, (d), (e), (f) 2344 Nitrided steel and ball tested at 5,10 and 15N.

The 3D surface profiles of wear scars of nitrided and bare samples tested under a dry sliding condition are shown in Figures 8, 9 and 10. Wear volumes of the wear scars were obtained by scanning all the wear scar surfaces with a confocal optical profilometer.

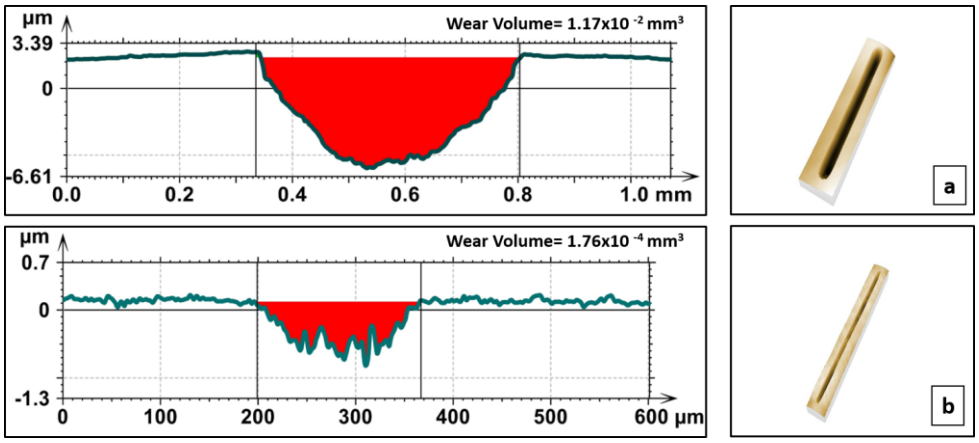

Figure 8. Optical profilometer images of the samples (a) 2344 bare steel and (b) 2344 nitrided steel at 5N.

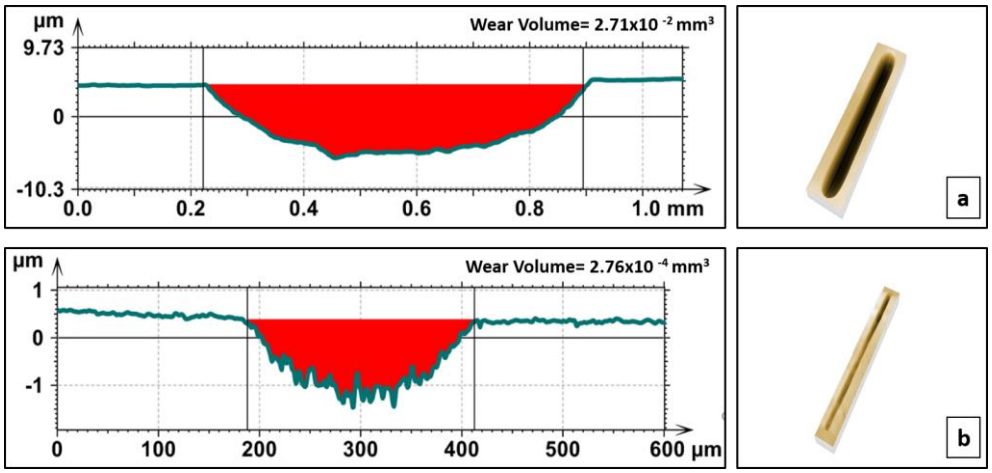

Figure 9. Optical profilometer images of the samples (a) 2344 bare steel and (b) 2344 nitrided steel at 10N.

Mountains map software was used to convert the wear volumes and wear scar cross-sections into numerical values and compare them. When the wear volumes are compared, positive the effect of nitriding can be seen on wear resistance of the bare steel. The wear volumes of nitrided samples were lower than bare steel. This difference in the wear volume of between bare steel and nitriding steel was observed to be approximately 5 times at 1.9 GPa contact pressure (15N).

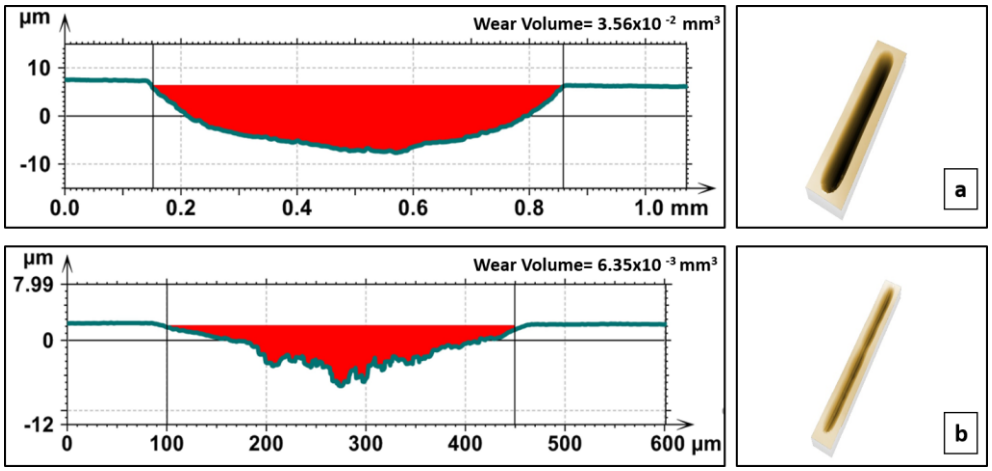

Figure 10. Optical profilometer images of the samples (a) 2344 bare steel and (b) 2344 nitrided steel at 15N.

Wear rates, W_R, were obtained by Archard's equation as shown in Eq. 2 and plotted in Figure 11.

$$W_R = \frac{\Delta V}{F_N \times L} \tag{2}$$

V (mm^3) is the wear volume, F_N (N) is the applied force and L (m) is the sliding distance at the eq(2) [24].

When looking at the 2344 bare steel sample wear rates were measured to be $2.35x10^{-5}$ $mm^3/N.m$, $2.71x10^{-5}$ $mm^3/N.m$, $2.37x10^{-5}$ $mm^3/N.m$ at 5, 10, 15N, respectively and 2344 nitriding sample wear rates were measured to be $3.53x10^{-7}$ $mm^3/N.m$, $2.76x10^{-7}$ $mm^3/N.m$, $4.23x10^{-6}$ $mm^3/N.m$ at 5, 10, 15N, respectively. Nitrided 2344 steel showed the best wear resistance with the $2.76x10^{-7}$ $mm^3/N.m$ at 10N [25].

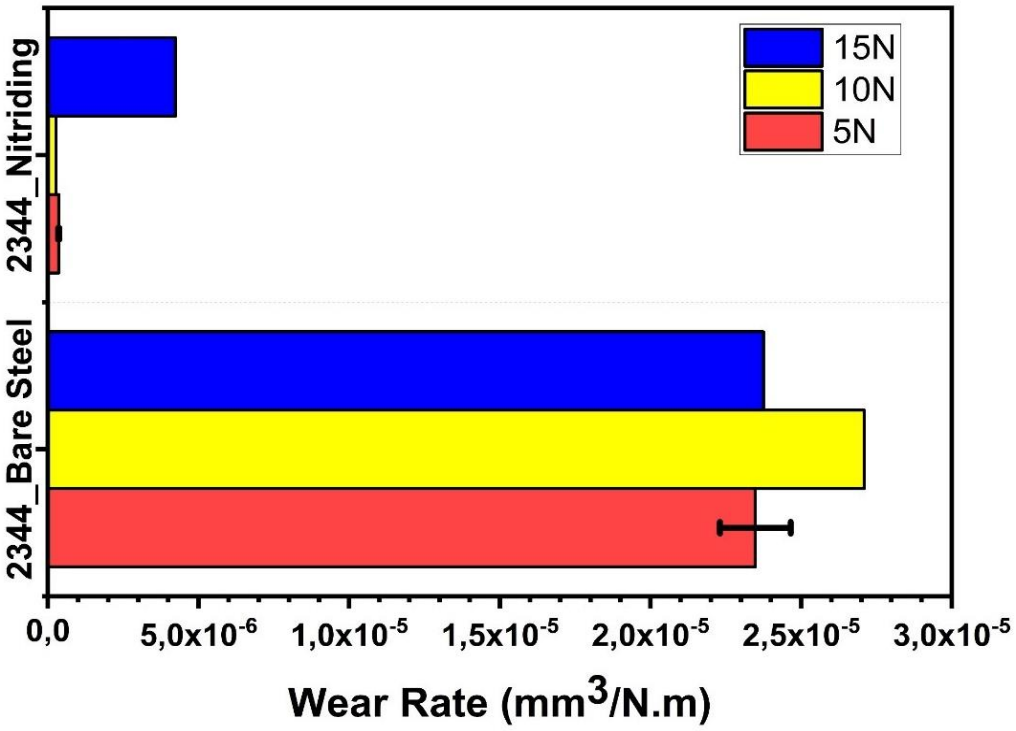

Figure 11. Wear rates of 2344 bare steel and 2344 nitrided steel at 5N, 10N, 15N.

Figure 12 and Figure 13 shows AFM topography analysis of abrasive wear scars of 2344 bare steel and nitride steel, respectively. Abrasive wear scars depths were 373, 614, and 512 nm at 5, 10, and 15N for 2344 bare steel. Abrasive wear scars depths were 238, 485, and 510 nm at 5, 10, and 15N for 2344 nitrided steel [26].

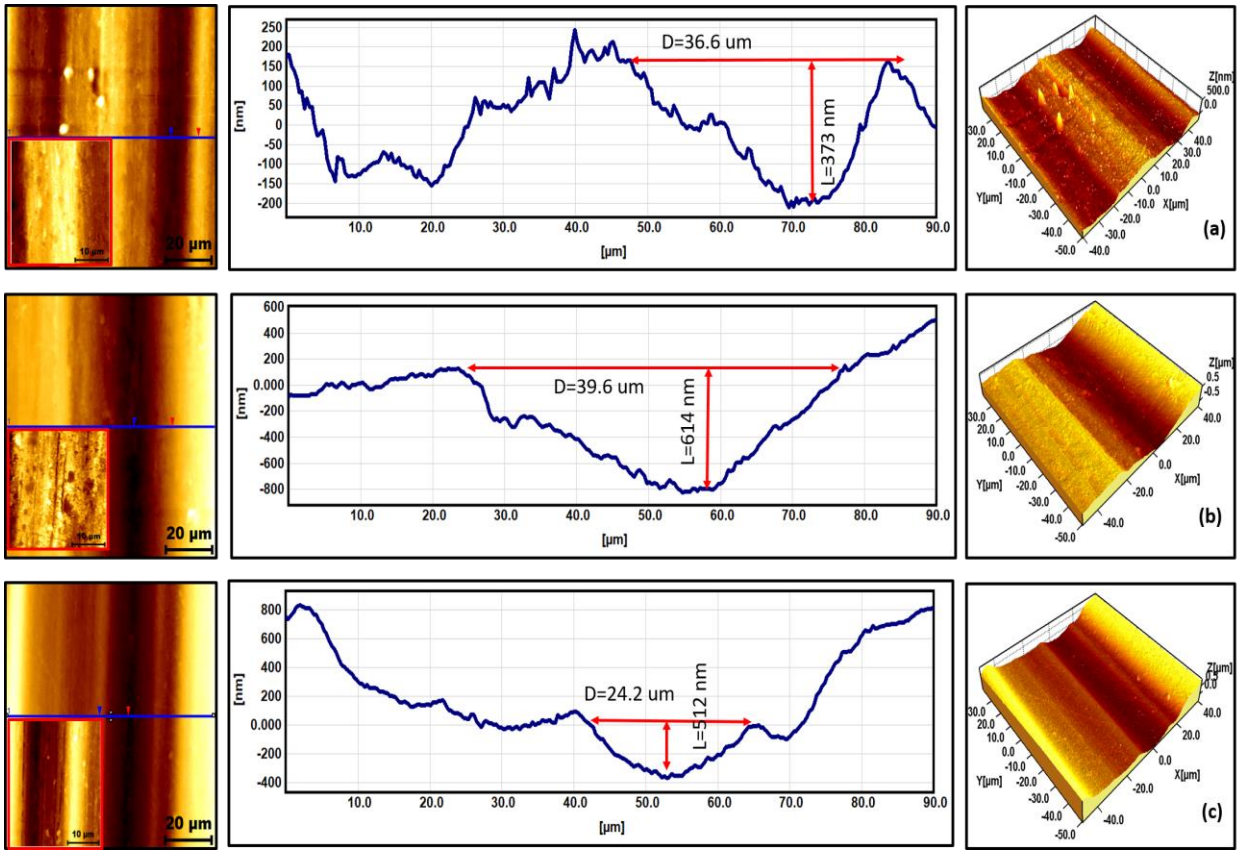

Figure 12. AFM analysis of the wear scars of 2344 bare steel (a) 5N, (b) 10N and (c) 15N.

It can be seen that the application of a higher load scales up the scratch depth. In addition, the nitrided sample has a lower wear scar depth than the bare steel sample. The wear scar depths in 10N and 15N loads have approximately the same values in both samples[27-28].

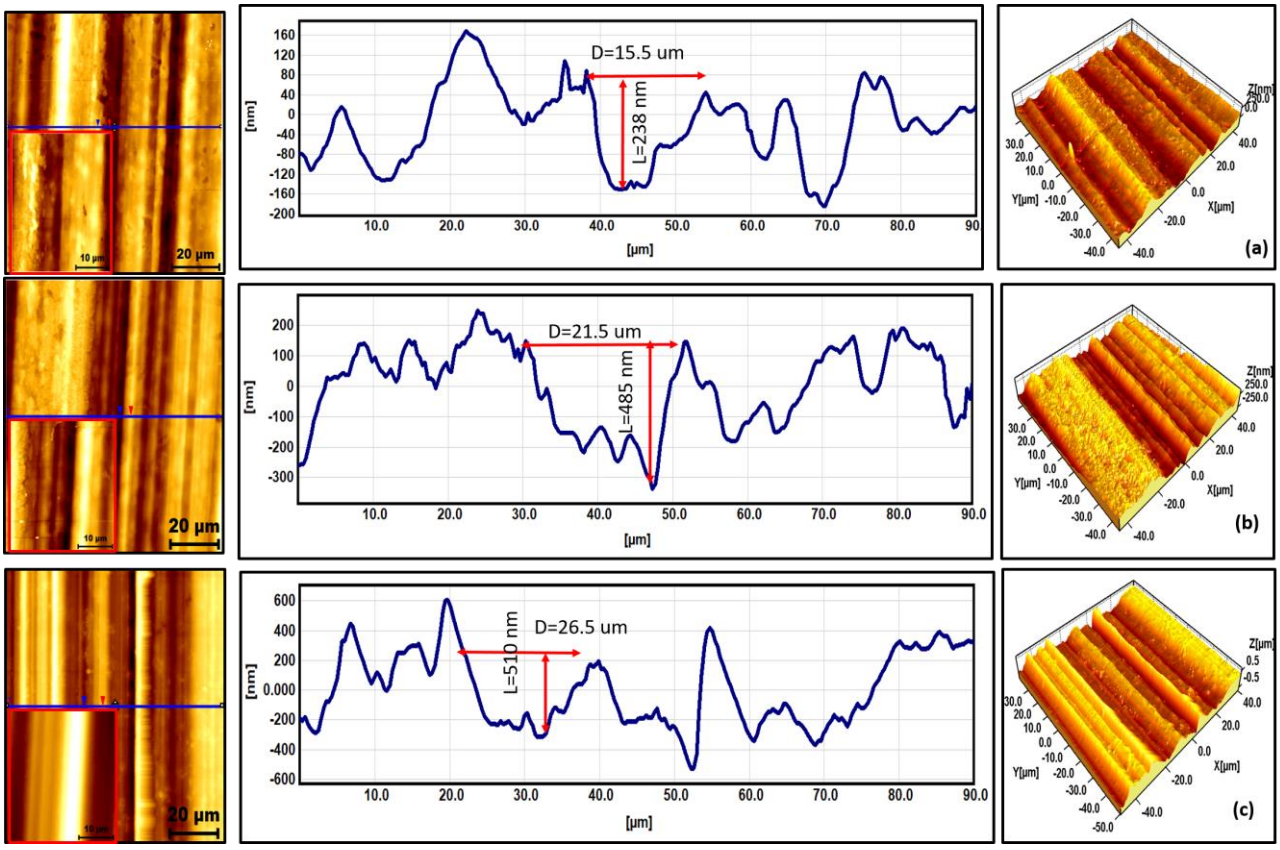

Figure 13. AFM analysis of the wear scars of 2344 nitrided steel (a) 5N, (b) 10N and (c) 15N.

3.3. Tribochemical Analysis of The Worn Surfaces

SEM/EDX results were shown in Figure 14. When the elemental composition of the 2344 bare steel wear scars is examined, the elements that constitute the chemical composition of 2344 steel and oxygen are determined. The reason for this is the oxide layer formed on the surface as a result of contact of the wearing surface with air during the wear test [10].

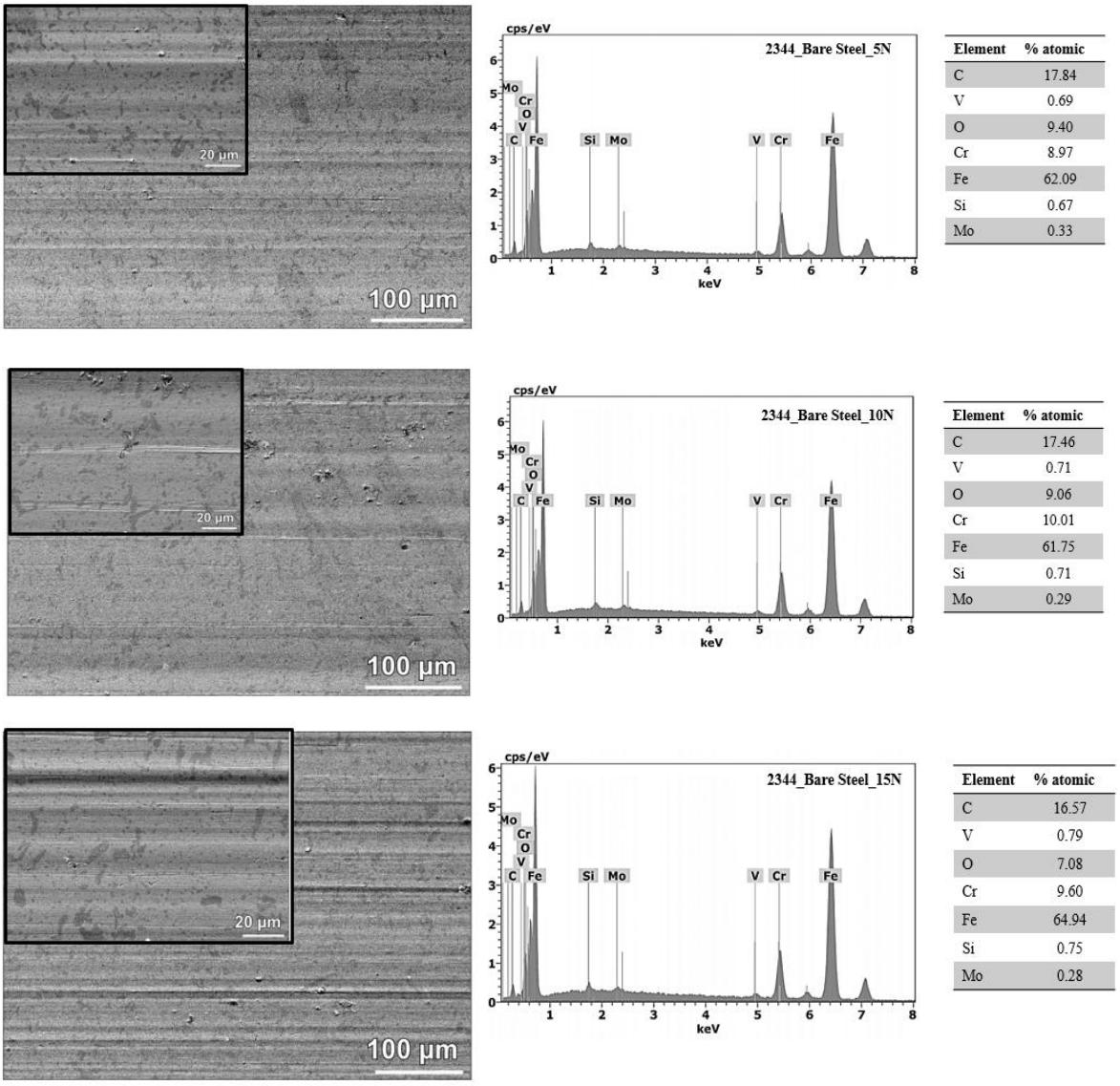

Figure 14. SEM/EDX analysis of the 2344 bare steel tested at 5N, 10N and 15N.

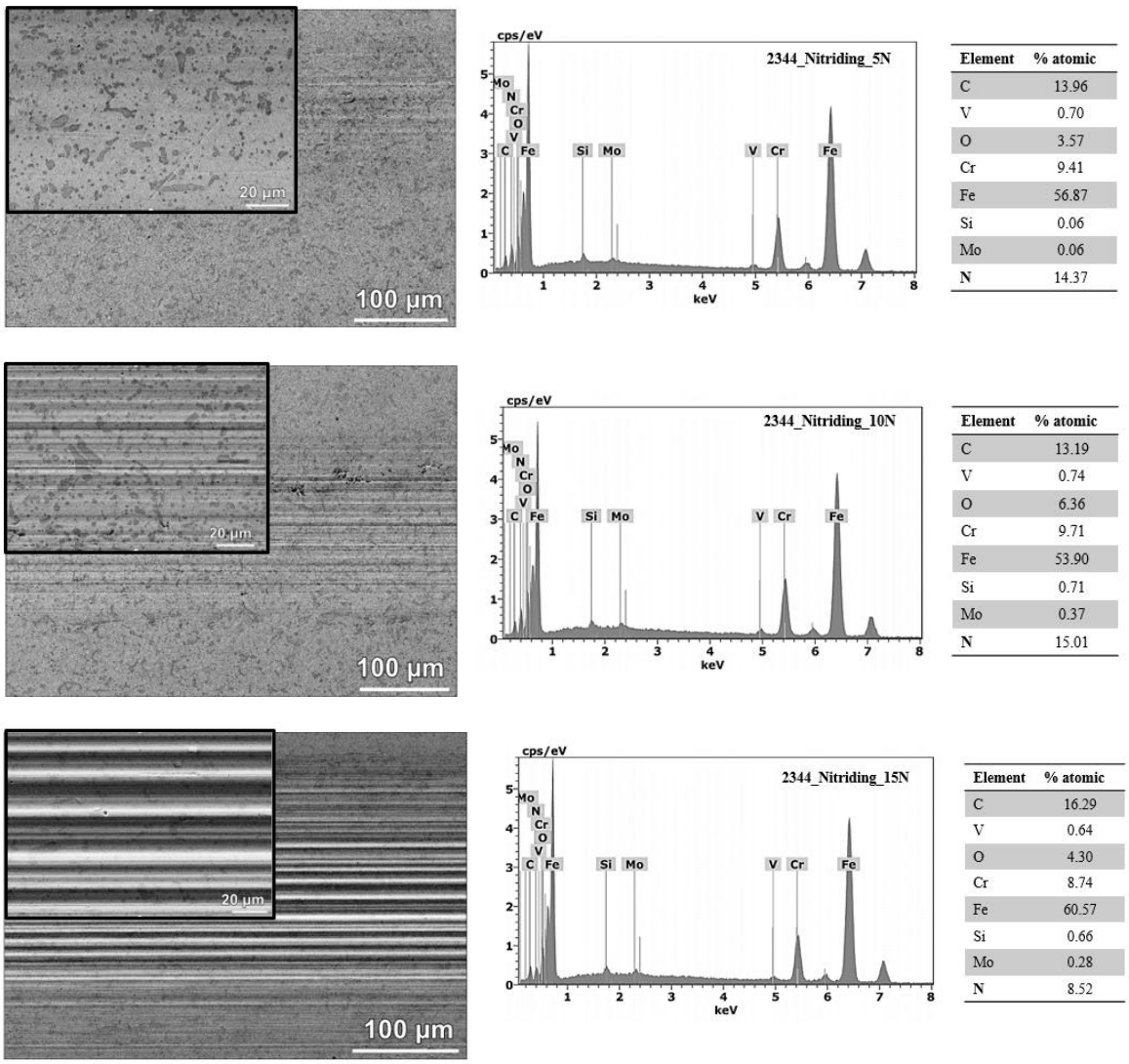

Element	% atomic
C	13.96
V	0.70
O	3.57
Cr	9.41
Fe	56.87
Si	0.06
Mo	0.06
N	14.37

Element	% atomic
C	13.19
V	0.74
O	6.36
Cr	9.71
Fe	53.90
Si	0.71
Mo	0.37
N	15.01

Element	% atomic
C	16.29
V	0.64
O	4.30
Cr	8.74
Fe	60.57
Si	0.66
Mo	0.28
N	8.52

Figure 15. SEM/EDX analysis of the 2344 nitrided steel tested at 5N, 10N and 15N.

2344 nitrided sample's SEM/EDX results were shown in Figure 15. When the SEM/EDX results of nitrided samples are examined, an expected increase in N percentage due to the nitriding process was observed. The higher level of Fe was detected with the load increase and the nitration layer decrease [16].

4. CONCLUSIONS

The mechanical and wear behavior of DIN 1.2344 hot-work tool steel, frequently used in the production area, is a significant research issue. The present study was performed to investigate the wear behavior of nitrided DIN 1.2344 hot work steel. The diffusion layers have been created as a result of the gas nitriding process in ammonia. Microscopic examinations exhibit that the microstructure varies from the surface to the core. The compound layer, diffusion zone, and core are illustrated in the optic microscope image of nitrided 2344 steel. The thickness of the diffusion zone was measured to be about 77 µm. The friction coefficient of the nitrided steel and non-nitrided 2344 steel increased in the early step of the wear tests. However, the friction coefficients of non-nitrided 2344 steel were higher than nitrided 2344 steel under all contact pressure. Wear scars analysis results indicated that the wear rate increased with a higher load at a constant sliding distance for both samples. The EDX analysis of nitride sample showed nitride precipitates exist within the grains and at the grain boundaries. Furthermore, Cr which is the base alloying element in DIN 2344 steel, has a comparatively intense chemical bond with nitrogen through the nitriding process. The consequence of the AFM analysis introduced that the abrasive wear scar depths of the nitrided sample were lower at 5N whereas similar depths were observed for at 10N and 15N. Herewith the wear resistance of steel was substantially advanced by the gas nitriding process. This work can also support the improvement and productive usage of hot work steel with these findings.

5. ACKNOWLEDGMENTS

The authors thank the support of the Scientific Research Projects Unit of Marmara University, Turkey for the funded project, Project no FEN-C-YLP-120619-0198 and Titanit Ultrahard PVD coatings company in Turkey.

REFERENCES

[1] Kostova, K.G., Uedaa, M., Lepienskyc, M., Soares Jr., P.C., Gomesa, G.F., Silvad, M.M., Reuther H. (2004). Surface Modification of Metal Alloys By Plasma Immersion Ion Implantation and Subsequent Plasma Nitriding. Surface and Coatings Technology, 186, 204–208.

[2] Castro, G., Fernández-Vicente, A., Cid, J. (2007). Influence of The Nitriding Time in The Wear Behavior of An AISI H13 Steel During A Crankshaft Forging Process. Wear, 263, 1375–1385.

[3] da Silva, L.L.G., Ueda, M., Nakazato, R. Z., (2007). Enhanced Corrosion Resistance of AISI H13 Steel Treated By Nitrogen Plasma Immersion Ion Implantation. Surface and Coatings Technology, 201, 8291–8294.

[4] Arif, A.F.M., Akhtar, S. S., Yilbas, B. S. (2010). Effect of ProcessVariables on Gas Nitriding of H13 Tool Steel With Controlled NitridingPotential. International Journal of Surface Science and Engineering, 4, 396–415.

[5] Rodrigo L.O. B., Heloise O. P., Vanessa S., Israel J.R. B., Silvia A.C. A., Fernando S. de S., Almir S., Carlos A. F., Cristiano G., (2010).Microstructure and Corrosion Behaviour of Pulsed Plasma-Nitrided AISI H13 Tool Steel. Corrosion Science, 52, 3133–3139.

[6] Yeh, S.-H., Chiu, L.-H., Chang, H. (2011). Effects of Gas Nitriding on the Mechanical and Corrosion Properties of SACM 645 Steel.Engineering, 3, 942–948.

[7] Rodríguez-Baracaldo, R., Benito, J. A., Puchi-Cabrera, E. S., Staia, M. H. (2007). High-Temperature Wear Resistance of (TiAl)N PVD Coatingon Untreated and Gas Nitrided AISI H13 Steel With Different Heat Treatments. Wear, 262, 380–389.

[8] Lampe, T., Eisenberg, S., Laudien, G. (1993). Compound LayerFormation During Plasma Nitriding and Plasma Nitrocarburising. Surface Engineering, 9, 69–76.

[9] Baranowska, J. (2010). Importance of Surface Activation for Nitrided Layer Formation on Austenitic Stainless Steel. Surface Engineering, 26,293–298.

[10] Birol, Y., Yuksel, B. (2012). Performance of Gas Nitrided and AlTiN Coated AISI H13 Hot Work Tool Steel in Aluminium Extrusion. Surface and Coatings Technology, 207, 461–466.

[11] Güven, Ş. Y., Delikanlı, K., Öncel, E. (2014). AISI 4140 ÇeliğineUygulanan İyon Nitrasyon Yüzey Sertleştirme İşleminin Yorulma Dayanımına Etkisi. SDU Teknik Bilimler Dergisi, 4, 29-39.

[12] Bayramoglu, M., Polat, H., Geren, N. (2008). Cost and Performance Evaluation of Different Surface Treated Dies for Hot Forging Process.Journal of Materials Processing Technology, 205, 394–403.

[13] Barrallier, L. (2015). Classical Nitriding of Heat Treatable Steel.Woodhead Publishing Limited, 393-412.

[14] Azadi, M., Rouhaghdam, A. S., Ahangarani, S., Mo, H. H. (2014). Mechanical Behavior of TiN / TiC Multilayer Coatings Fabricated By Plasma Assisted Chemical Vapor Deposition on AISI H13 Hot Work Tool Steel. Surface and Coatings Technology, 245, 156–166.

[15] Li, K. Y., Xiang, Z. D. (2010). Increasing Surface Hardness of Austenitic Stainless Steels By Pack Nitriding Process. Surface and Coatings Technology, 204, 2268–2272.

[16] Cui, X. H., Wang, S. Q., Wei, M. X., Yang, Z. R. (2011). Wear Characteristics and Mechanisms of H13 Steel with Various Tempered Structures. 20, 1055–1062.

[17] Arif, A.F.M., Akhtar, S. S., Yilbas, B. S. (2012). Influence of Multiple Nitriding on The Case Hardening of H13 Tool Steel: Experimental and Numerical Investigation. International Journal of Advanced Manufacturing Technology, 8, 57–70.

[18] Akhtar, S. S., Arif, A.F.M., Yilbas, B. S., Sheikh, A.K. (2010).Influence of Surface Preparation on the Kinetics of Controlled Gas-Nitrided AISI H13 Steels Used in Extrusion Dies, 19, 347–355.

[19] Greenwood, J. A. (1985). Formulas for Moderately Elliptical Hertzian Contacts, Journal of Tribology, 107, 501–504.

[20] Jordan, D., (2010). Controlling Compound (White) Layer Formation During Vacuum Gas Nitriding. Solar Atmospheres Inc., 1-20.

[21] Bahrami, A., Anijdan, S. H. M., Golozar, M. A., Shamanian, M., Varahram, N. (2005). Effects of Conventional Heat Treatment on Wear Resistance of AISI H13 Tool Steel. Wear, 258, 846–851.

[22] Jacobsen, S. D., Hinrichs, R., Aguzzoli, C., Figueroa, C. A., Baumvol, I. J. R., Vasconcellos, M. A. Z. (2016). Influence of Current Density on Phase Formation and Tribological Behavior of Plasma Nitrided AISI H13 Steel. Surface and Coatings Technology, 286, 129–139.

[23] Gasem, Z. M. (2013). Cracking in A Multiple Gas-Nitrided H13 Aluminum Extrusion Mandrel. Engineering Failure Analysis Journal, 31,68–75.

[24] Yang, K., Shi, X., Zhai, W., Mahmoud Ibrahim, A. M. (2015). WearRate of A Tial Matrix Composite Containing 10 Wt% Ag Predicted Using The Newton Interpolation Method. RSC Advances, 5, 67102-67114.

[25] Telasang, G., Dutta Majumdar, J., Padmanabham, G., Manna, I. (2015). Wear and Corrosion Behavior Laser Surface Engineered AISI H13 Hot Working Tool Steel. Surface and Coatings Technology 261, 69–78.

[26] Jeong, B. Y., Kim, M. H. (2001). Effects of Pulse Frequency and Temperature on The Nitride Layer and Surface Characteristics of Plasma Nitrided Stainless Steel. Surface and Coatings Technology, 137, 249–254.

[27] Fernandes, F. A. P., Heck, S. C., Picone, C. A., & Casteletti, L. C. (2020). On the wear and corrosion of plasma nitrided AISI H13. Surface and Coatings Technology, 381, 125216.

[28] Miyamoto, J., Abraha, P. (2019). The effect of plasma nitriding treatment time on the tribological properties of the AISI H13 tool steel.Surface and Coatings Technology, 375, 15–21.

Journal of Naval Sciences and Engineering
2020, Vol. 16, No.1, pp.71-83
Electric-Electronic Engineering/Elektrik-Elektronik Mühendisliği

RESEARCH ARTICLE

INVESTIGATION OF THE SPUTTERING CONDITIONS ON THE DEPOSITION OF THE NbN THIN FILMS ONTO GLASS AND Si/SiO SUBSTRATES

Atılgan ALTINKÖK[1]

[1]*National Defense University, Turkish Naval Academy, Electrical and Electronics Engineering, Istanbul, Turkey,*
aaltinkok@dho.edu.tr; ORCID: 0000-0002-0548-4361

Date of Receive: 06.03.2020 **Date of Acceptance: 26.03.2020**

ABSTRACT

NbN thin films are very useful superconducting materials for the electronic devices. Using sputter deposition technique is a cheap alternative to produce of NbN thin films on glass or SiO for the technology applications. The NbN films was coated on glass and SiO/Si substrates by DC magnetron sputtering technique. Pure Nb target was used the production of NbN thin films in different compositions of Argon and nitrogen gases. The effects of different substrate temperatures, sputtering power and, various ratios of Nitrogen/Argon gases were investigated on Superconducting Critical Temperature (Tc). It is seen that increasing the substrate temperature or sputtering power resulted in increased on the Tc. Thereby optimum condition values are deduced by the Residual Resistance Ratio (RRR) calculation and resistance-temperature (R-T) curves. It is observed that the substrate temperature and the flux of nitrogen gas effect (111) preferential orientation during the deposition, whereas the critical temperature of the thin films is affected by the of deposition chamber vacuum. Tc is also highly dependent on the Nitrogen and Argon pressures on sputtering deposited NbN films.

Keywords: *Transition Temperature, Niobium Nitride (NbN), Thin Films, Residual-Resistance Ratio, Superconductivity.*

Investigation of The Sputtering Conditions On The Deposition of The NbN Thin Films Onto Glass and Si/SiO Substrates

CAM VE Si/SiO ALTTAŞ ÜZERİNE KAPLANAN NbN İNCE FİLMLERİN KAPLAMA KOŞULLARININ ARAŞTIRILMASI

ÖZ

NbN ince filmler elektronik cihazlar için çok kullanışlı süper iletken malzemelerdir. Püskürtme biriktirme tekniğini kullanması teknoloji uygulamaları için cam veya SiO üzerinde NbN ince filmlerin üretilmesi için ucuz bir alternatiftir. . Bu çalışmada, NbN ince filmler, reaktif magnetron püskürtme yöntemi ile cam, Si ve SiO alt tabakaları üzerine kaplanmıştır. Saf Nb metali, Argon ve azot gazlarının farklı karşım oranlarında NbN ince filmlerinin üretimi için kullanılmıştır. Çeşitli alttaş sıcaklıkları, püskürtme gücü ve Argon / Azot gazı oranının süperiletken geçiş sıcaklığı (T_c) üzerine etkileri araştırılmıştır. Alttaş sıcaklığının veya püskürtme gücünün arttırılmasının T_c'yi de arttığı görülmüştür. Bunun sonunda optimum sıcaklık değerleri, direnç-sıcaklık (R-T) eğrileri ve Artık Direnç Oranı (RRR) hesaplaması yardımı ile bulunmuştur. Kaplama sırasındaki alttaş sıcaklığının ve azot gazı akış değerlerinin tercih edilen yönlendirmeyi güçlü bir şekilde etkilediği gözlenirken, ince filmlerin kritik sıcaklığı orijinal vakumun kalitesinden etkilenmektedir. Ayrıca T_c üretilen NbN filmlerinin kalitesi kaplama işlemi süresindeki Azot ve Argon basınçlarına da oldukça bağımlıdır.

Anahtar Kelimeler: *Kritik Sıcaklık, NbN, İnce Film, Kalıntı Direnç Oranı, Süperiletkenlik.*

1. INTRODUCTION

The nitrite thin film coating is used in the field of different technologies. However, NbN thin films produced by sputtering on Si or SiO2 substrate are more attractive among other studies due to their low cost and easy accessibility for the production of high-density integrated circuits. NbN thin films can produced by reactive DC magnetron sputtering [1-4], ion beam deposition [5, 6], pulse laser deposition [7, 8] metal organic chemical deposition (MOCVD) [9]. In order to obtain NbN thin films with good superconducting properties, it is necessary to define the appropriate value production conditions well, which is possible with detailed studies on the effects of conditions in the deposition process.

Previous works [10], on the development of superconductivity properties of NbN thin films, proved that the partial nitrogen pressure increase in the Argon-Nitrogen (Ar / N_2) gas mixture provides an increase in the N/Nb ratio in NbN thin films. Competition among researchers is still ongoing to find the effective mechanism that primarily suppresses superconducting critical temperature (T_c) and to increase in the T_c of NbN films. The effects of parameters such as Ar and N_2 pressures, film deposition time, and substrate selection on the NbN thin films should be investigated in more detail.

In the past, studies were carried out on the improvement of T_c at optimized production conditions. For example, the influence of the N_2 partial pressure ratio on the film produced at room temperature was studied by Z. Wang et al. [11], at the same time the effect of the temperature of the substrate and sputtering power were investigated by S. Chockalingam et al. [12]. In addition, the effects of film thickness on T_c of NbN is summarized in [13] and [14].

In this study, some basic measurements were made about the production of NbN thin films and the change in superconductivity transition temperature. NbN films were produced in ultra high vacuum system with DC reactive magnetron sputtering technique. The effect of different rates of Ar and N_2 gases on glass and Si / SiO_2 on two different substrate of T_c were investigated. T_c was found in the range of 4.5-8.5 K and 10.1-14.7 K for Nb and NbN thin films, respectively depending on the sputtering conditions.

The highest T_c of the NbN is 14.7 K on the Si/ SiO_2 substrate at 300 W sputtering power. According to our results, Si/ SiO_2 substrate improves superconducting properties of the superconducting thin films. Residual-resistivity ratio (RRR) is calculated for the thin films and the flux of N_2 have a strong effect on RRR of the thin films.

2. MATERIALS AND METHOD

NbN films were produced by reactive DC magnetron sputtering method in cryo and turbomolecular pumped chamber where base pressure prior to sputtering was below $2x10^{-6}$ Pa. The NbN films were deposited using a 99.95% pure Nb target from Kurt Lesker Co. with a diameter of 3 inch in an argon and nitrogen mixture atmosphere onto glass and thermally oxidized Si (Si/SiO_2) substrates. The pure Argon (99.999%) partial pressure was kept at 0.3 Pa and the nitrogen (99.99%) various nitrogen pressures. The nitrogen concentration in the mixed gases, which is defined as the nitrogen partial pressure divided by the total pressure of 1.0 Pa, which can be changed from 0% to 100%. In this study, partial pressure of nitrogen was varied from %15 to %20. Argon flow rate was optimized to produce stress free NbN thin films and the Nitrogen flow rate to reach maximum critical temperature. Gas pressures were precisely measured by digital mass flow meter (Sierra Mass Flow Meter-Smarttrek100). During deposition the flow rate (Ar: N_2) for glass substrate was set to 40: 9.5 sccm and Si / SiO_2 substrate (Ar: N_2) 40: 7.06 sccm. To prevent surface impurities in NbN films to be prepared, pre-sputtering was applied to the Nb target for 20 minutes by closing the cover in front of the substrate prior to the deposition process. The power of DC power supply was kept at 190 and 300 W, respectively. The distance between the target and the substrate in the chamber is 80 cm to achieve the highest deposition rate and the deposition rate was 6.8 nm/s for every sample. Thin film thickness was measured calibrated with a computer-controlled quartz crystal thickness monitor. Then, these thicknesses were confirmed by measuring with a profilometer (Bruker DXT stylus).

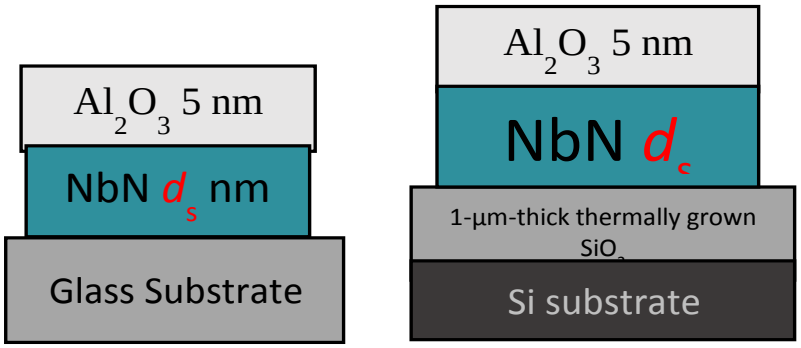

Figure 1. Schematic diagram of the NbN films onto a) glass b) Si/SiO2 substrates.

Figure 1. shows the schematic diagram of the thin films which their surfaces were covered with a buffer layer Al_2O_3 of 5 nm thick to prevent the samples from being exposed to external influences and being degraded. The heater current is held constant for all thin film samples to heat the substrate and the substrate temperature was T_s = 450 ^oC.

The thin films electrically characterized by the standard 4-point method. Here, four connections made as two for voltage and two for current terminals. The voltage and current terminals were connected using indium with 0.5 mm diameter copper wire. The temperature of the samples was recorded by a calibrated RuO thermometer.

3. RESULTS AND DISCUSSION

Table 1 shows the variation critical transition temperature (T_c) of the NbN thin film deposited on the glass substrate at 450 ^oC for different thicknesses

Table 1. Variation of the critical temperature by thickness.

NbN Film Thickness (nm)	T_c **(K)**	**RRR** ρ_{300}/ρ_{Tc}	**Argon Flux (sscm)**	**N_2 Flux (sscm)**	**Partial pressure ratio % N_2**
20	10.1	0.90	40	9.5	19.2
50	10.3	0.93	40	9.5	19.2
100	12.0	0.95	40	9.5	19.2
150	13.0	0.94	40	9.5	19.2

As seen in the table 1, the N_2 partial pressure has a value of 19.2% in total pressure. The reactive DC sputtering power is 190, used for the deposition of the NbN films onto glass substrates.

Here, the calculated RRR value is the ratio of the resistivity at 300 K to resistivity at 10 K. RRR value shows the level of the impurity. High RRR value implies high material purity for re-crystallized material. Niobium nitrate thin films can be characterized by RRR as the first criterion of the level of purity. This is easier and faster way when it is compared to thermal conductivity. The results in the table 1 show that increasing the thickness values improves the superconductivity properties of NbN thin films at optimum N_2 and Ar pressure on the glass substrate.

Figure 2 shows the variation of the thickness of the films produced on the glass substrate. Although the film, has thickness of 150 nm, gives the

highest superconductivity temperature (T_c = 13 K), the RRR value slightly decreases.

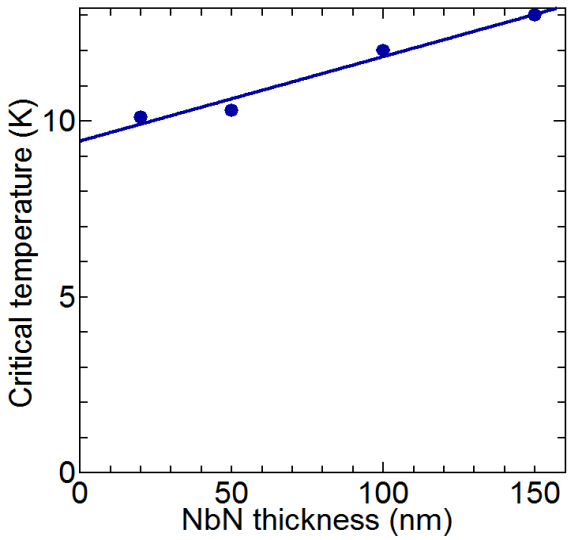

Figure 2. The thickness dependence of critical temperature (T_c).

This decrease in the RRR implies that when the superconductivity is improved on the films, the film quality may be poor. Changes in the grain structure of the films occurred by the deposition of the thicker thin films. In the study [15], the change in film quality is attributed to related the dependence of the T_c and RRR is connected the grain boundaries and scattering in point defects. For example, changes in the homogeneity of the thin film may cause this behavior. It has also been reported [1] that small particle size causes lower T_c values.

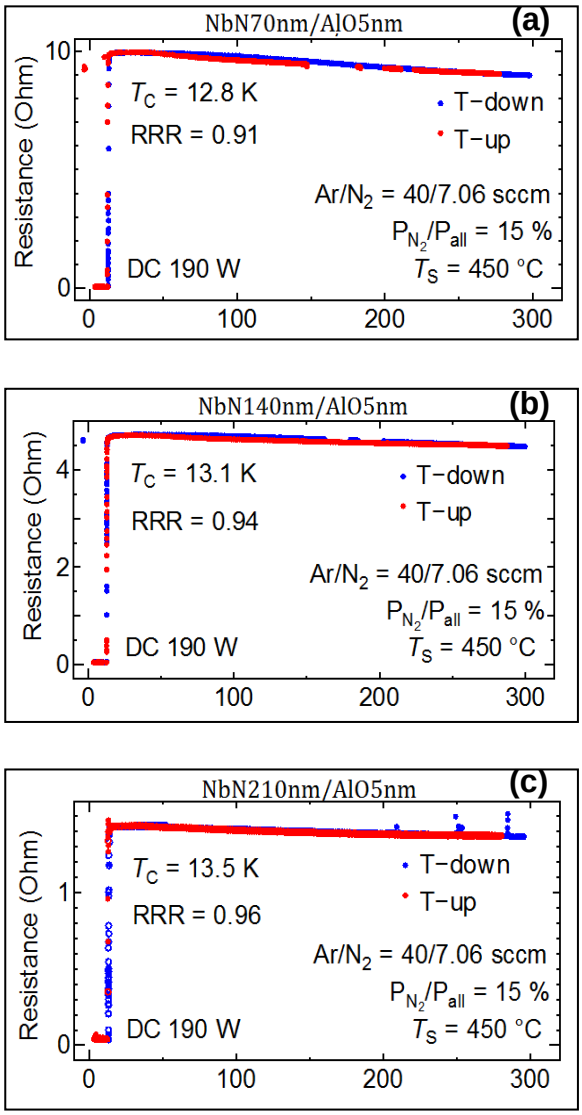

Figure 3. The resistance of NbN films as a function of temperature; a) 70 nm, b) 140nm, c) 210nm thickness.

Deposition of the NbN thin films on Si / SiO_2 substrates significantly changes the RRR and T_c values associated with film quality, despite the reduction of partial pressure N_2 gas and DC sputtering power. It is shown that how changes critical temperature and RRR values in detail for 190 W DC sputtering power, which observed highest T_c is 13.5 K, in the Figure 3.

The N_2 and Ar gas flux ratios, T_c and RRR variations for the films produced onto Si / SiO_2 substrate are given in table 2.

Table 2. Variation of the critical temperature by thickness and sputtering power.

NbN Film Thickness (nm)	**T_c (K)**	**RRR**	**Argon Flux (sscm)**	**N_2 Flux (sscm)**	**Partial pressure ratio % N_2**	**Sputter Power (W)**
70	12.8	0.91	40	7.06	15	190
140	13.1	0.94	40	7.06	15	190
210	13.5	0.96	40	7.06	15	190
210	12.7	0.94	40	7.06	18	300
210	14.7	0.95	40	7.06	19	300

As shown in Fig. 4. the highest T_c is measured as 14.7 K in our work, whereas an argon flow of 40 sccm, a partial N_2 pressure of 19% and a power of sputter of 300 W. Thus we conclude that critical temperature improved with increasing N_2 partial pressure and reaches a highest value. Especially, the effect of N_2 partial pressure on T_c at 300 W is clearly visible for this study.

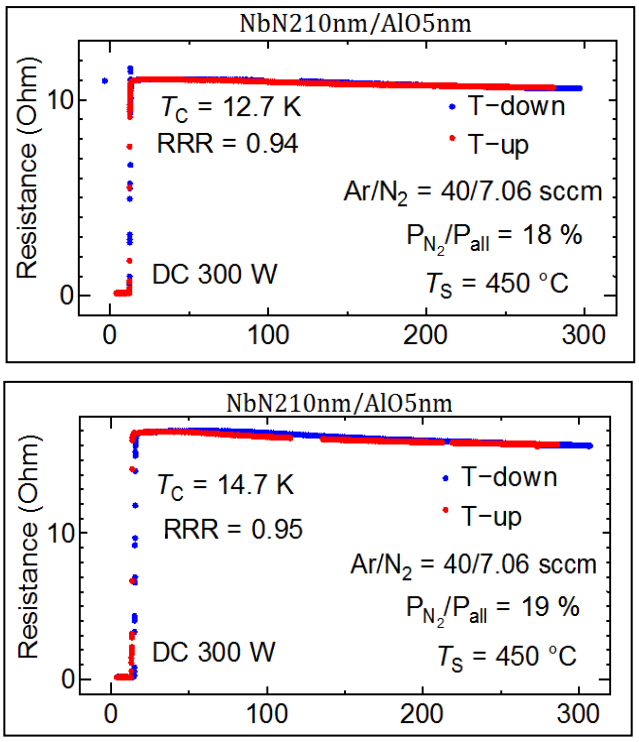

Figure 4. The resistance of NbN films as a function of temperature.

4. CONCLUSION

In this study, it is observed that with the increase in the substrate temperature and sputtering power and occasioned increase on the transition temperature (T_c) of the superconducting NbN thin films. A maximum value of T_c (14.7 K) is measured at 40/7.06 Ar/N_2 pressure ratio, 15% partial pressure of N_2 and 450 ^oC substrate temperature while the minimum is 12.7 K. These results are also routinely reproducible. The best thin films production parameters are calculated via Residual-Resistance Ratio and R-T curves. Then, it is conclude that the increase in temperature of substrate results in favor of critical superconducting temperature. It is also shown that T_c of the NbN films highly depends on the stream of N_2 and Ar gases.

5. ACKNOWLEDGEMENTS

The author would like to thank Dr. Yota TAKAMURA for the NbN thin film samples prepared by sputtering technique.

REFERENCES

[1] M.S. Wong, W.D. Sproul, X. Chu, S.A. Barnett, (1993). Reactivemagnetron sputter deposition of niobium nitride films, J. Vac. Sci. Technol. A: Vacuum, Surfaces, and Films, Vol. 11, No. 4, pp. 1528-1533.

[2] S. K. Kim, B. C. Cha, and J. S. Yoo, (2004). Deposition of NbN thin films by DC magnetron sputtering process, Surface and Coatings echnology,Vol. 177-178, pp. 434–440.

[3] J. J. Olaya, S. E. Rodil, and S. Muhl, (2008). Comparative studyof niobium nitride coatings deposited by unbalanced and balanced magnetron sputtering, Thin Solid Films, Vol. 516, No. 23, pp. 8319–8326.

[4] Kulwant Singh, A. C. Bidaye, and A. K. Suri C. S. Sandu, (2011). Magnetron Sputtered NbN Films with Nb Interlayer on Mild Steel, International Journal of Corrosion, Vol. 2011, pp. 1-11.

[5] Hoshi Y., Terada N., Naoe M., Yamanaka S., (1984). Fabrication of High T_c NbN Films by Ion Beam Deposition Technique, In: Clark A.F., Reed R.P. (Eds.) Advances in Cryogenic Engineering Materials. Advances in Cryogenic Engineering, Vol. 30. Springer, Boston, MA.

[6] M Kidszun, R Hühne, B Holzapfel and L Schultz, (2011). Ion-beam-assisted deposition of textured NbN thin films, Supercond. Sci. Technol. 23, pp. 025010-025018.

[7] G. Cappuccio, U. Gambardella, A. Morone, S. Orlando, and O. P. Parisi, (1997). Pulsed laser ablation of NbN/MgO/NbN multilayers, Applied Surface Science, Vol. 109, pp. 399–402.

[8] Y. Ufuktepe, A.H. Farha, S.I. Kimura, T. Hajiri, K. Imura, M.A.Mamun, F. Karadag, A.A. Elmustafa, H.E. Elsayed-Ali, (2013). Superconducting niobium nitride thin films by reactive pulsed laser deposition, Thin Solid Films, Vol. 545, pp. 601-607.

[9] M. Benkahoul, E. Martinez, A. Karimi, R. Sanjinés, F. Lévy,(2004). Structural and mechanical properties of sputtered cubic and hexagonal NbNx thin films, Surf. Coat. Technol., 180-181, pp. 178-183.

[10] Z. Wang, A. Kawakami, Y. Uzawa, B. Komiyama, (1996). Superconducting properties and crystal structures of single-crystal niobium nitride thin films deposited at ambient substrate temperature, J. Appl. Phys., 79, pp. 7837-7842.

[11] S. Chockalingam, M. Chand, J. Jesudasan, V. Tripathi, P. Raychaudhuri, (2008). Superconducting properties and Hall effect of epitaxial NbN thin films, Phys. Rev. B., 77, pp. 214503.

[12] L. Kang, B. B. Jin, X. Y. Liu, X. Q. Jia, J. Chen, Z. M. Ji, B. G. Wang, (2011). Suppression of superconductivity in epitaxial NbN ultrathin films, Journal of Applied Physics, 109(3), pp. 033908.

[13] S. Ezaki, K. Makise, B. Shinozaki, T. Odo, T. Asano, H. Terai, Z. Wang, (2012). Localization and interaction effects in ultrathin epitaxial NbN superconducting films, Journal of Physics. Condensed Matter: An Institute of Physics Journal, 24(47), pp. 475702.

[14] C. S. Sandu, M. Benkahoul, M. Parlinska-Wojtan, R. Sanjin´es, and F. L´evy, (2006). Morphological, structural and mechanicalproperties of NbN thin films deposited by reactive magnetronsputtering, Surface and Coatings Technology, Vol. 200, No. 22- 23, pp. 6544–6548.

[15] R. Sanjinés, M. Benkahoul, C.S. Sandu, P.E. Schmid, F. Lévy, (2006). Electronic states and physical properties of hexagonal β-Nb2N and δ′-NbN nitrides, Thin Solid Films, Vol. 494, 1-2, pp. 190-195.

JOURNAL OF NAVAL SCIENCES AND ENGINEERING (JNSE)
PUBLISHING RULES

Submission of Papers: Manuscripts submitted to the journal should not be published elsewhere or sent for publication. Authors are requested to submit an electronic copy of their original works to given "system address" (preferred) or one hard-copy to mail address and a soft-copy to "e-mail address" below. It is necessary for the authors to submit their manuscripts together with the "Copyright Release Form". "Copyright Release Form" can be downloaded from the web page ("Copyright" page) of JNSE.

System Address:
http://dergipark.gov.tr/jnse

Address:
Doç.Dr. Ertan YAKICI
Milli Savunma Üniversitesi
Barbaros Deniz Bilimleri ve Mühendisliği Enstitüsü
Deniz Harp Okulu Yerleşkesi
34942 Tuzla/ İSTANBUL/TÜRKİYE

E-mail: jnse@dho.edu.tr

Types of Contributions: The journal publishes original papers, review articles; technical notes; short communications; book reviews; letters to the editor; extended reports of conferences and meetings.

Manuscript Evaluation Process: The Peer Review Step:

- The content and the layout format of manuscript are examined and the originality of study is checked by iThenticate software programme.
- The language and correlation of the abstract with Turkish part are checked.
- Manuscript which has a similarity index above 40% is rejected. Manuscript, which has a similarity index between 20% and 40% (not more than 4% from a single source), which is not appropriate for the writing rules of JNSE or which needs correction in English and Turkish abstract, is informed to the author and it is requested to revise the manuscript by the author within "two weeks". Otherwise, the manuscript is considered as a withdrawal.

Our journal uses **double-blind** review, which means that both the reviewer and author identities are concealed from the reviewers, and vice versa, throughout the review process. So, the uploaded manuscript does not contain the name, address and affiliation of author(s). The manuscript evaluation steps are as follows;

- Editor is assigned by the Editor in Chief
- The relevant reviewers are assigned by the Editor
- As a result of the reviewer's evaluation, the manuscript may be rejected, accepted or a correction for the manuscript may be requested.
- If the negative feedback is given by major number of the reviewers the process is terminated and the article is rejected.
- If major/minor revisions are required for the manuscript, the author has to do this revision according to the reviewers' comments in "three weeks".
- If the revision is accepted by the reviewers, the article is accepted.

The workflow diagram for the evaluation process can be accessed from the web page of the journal.

The articles submitted to JNSE to be published are free of article submission, processing and publication charges. The accepted articles are published **free-of-charge** as online from the journal website and printed.

DENİZ BİLİMLERİ VE MÜHENDİSLİĞİ DERGİSİ (DBMD)
YAYIN KURALLARI

Yazıların Gönderilmesi: Dergiye gönderilen makaleler başka bir yerde yayımlanmamış ya da yayımlanmak üzere gönderilmemiş olmalıdır. Yayımlanması istenilen yazılar aşağıda verilen adresten sisteme yüklenmeli (tercih edilen) veya aşağıdaki adrese bir kopya kâğıda basılı olarak, aynı zamanda e-mail adresine de dijital olarak gönderilmelidir. Dergimize makale gönderen yazarların makaleleriyle birlikte "Yayın Hakkı Devir Formu"nu da göndermeleri gerekmektedir. "Yayın Hakkı Devir Formu"na DBMD web sayfasındaki "Telif Hakkı" sayfasından erişilebilmektedir.

Sistem Adresi:
http://dergipark.gov.tr/jnse

Adres:
Doç.Dr. Ertan YAKICI
Barbaros Deniz Bilimleri ve Mühendisliği Enstitüsü
Deniz Harp Okulu Yerleşkesi
34942 Tuzla/ İSTANBUL/TÜRKİYE

E-mail: jnse@dho.edu.tr

Yazı Türleri: Dergide; orijinal yazılar, derlemeler, teknik notlar, kitap incelemeleri, editöre mektuplar ile konferans ve toplantıların genişletilmiş raporları yayımlanır.

Yazıların Değerlendirilme Süreci: Makalenin Ön Kontrol Süreci:

- Makalenin içeriği ve yazım formatı incelenir ve iThenticate programı ile benzerlik taraması yapılır.
- Makalenin İngilizce özetinin, Türkçe öz ile uygunluğu ve yazım dili kontrol edilir.
- Benzerlik oranı %40'ın üzerinde olan makale reddedilir. Benzerlik oranı %20 ile %40 arasında olan (tek bir kaynakla benzerlik %5'ten fazla olmamalıdır), yazım formatına uymayan ya da İngilizce ve Türkçe özetinde düzeltme gereken makale yazara bildirilir ve "iki hafta" içerisinde makalenin düzeltilmesi istenir. Aksi takdirde makale çekilmiş kabul edilir.

Dergimiz, makale değerlendirme sürecinde **çift-kör** hakemlik sistemini kullanmaktadır. Buna göre değerlendirme sürecinde hakem ve yazarlar birbirlerinin bilgilerini görememektedir. Bu yüzden, yüklenen ön yükleme formatında yazar(lar)ın isim, adres ve bağlı olduğu kuruluş(lar) yer almamaktadır. Makale değerlendirme sürecindeki adımlar aşağıdaki gibidir;

- Baş editör tarafından makaleye editör atanır.
- Editör makale için hakemleri atar.
- Hakem değerlendirmesi sonucunda makale reddedilebilir, kabul edilebilir veya makalenin düzeltilmesi istenebilir.
- Hakem görüşlerinin çoğunluğu doğrultusunda makale ret edilmişse süreç sonlandırılır ve makale reddedilir.
- Makale için düzeltme istenirse hakem görüşleri doğrultusunda yazarın düzeltmeleri en geç "üç hafta" içerisinde yapması istenir.
- Makale kabul alırsa düzenleme aşamasına geçilir.

Değerlendirme sürecine ilişkin iş akış sürecine, dergi web sayfasından erişilebilir.

DBMD'ye yayımlanmak üzere gönderilen makaleler; makale gönderim, işlem ve yayın ücretinden muaftır. Kabul edilen makaleler, **ücretsiz** olarak basılı şekilde ve dergi web sayfasından çevrimiçi (on-line) olarak yayınlanmaktadır.

JOURNAL OF NAVAL SCIENCES AND ENGINEERING (JNSE) WRITING RULES

General: Manuscripts must be prepared in MS Word, single-spaced with justify. Font: Times New Roman, 12 points. Margins: left 4,5 cm- right 3,5 cm, top 5 cm- bottom 7 cm, header 3,25 cm- footer 6 cm, gutter 0. Paper type: A4. Page numbers should be on the middle of bottom of page with -1-, -2-, -3- etc format. Using footnotes is not allowed.

Body of Text: Follow this order when typing manuscripts: Title, Authors, Abstract, Keywords, Title (Turkish), Abstract (Turkish), Keywords (Turkish), Main Text, Appendix (if any), References.

Title: Title should reflect objectives of the paper clearly, be easily understandable and not exceed 15 words.

Abstracts: Each paper should have an abstract with 100-200 words and have a structured form, i.e. standard structure of an article (background, purpose, material and methods used, results, conclusion).

Paper Length: The manuscript should be minimum 2000 words or 5 pages, maximum 7000 words or 25 pages including references.

Keywords: Author must provide some keywords (between 3 and 5) that will be used to classify the paper.

Unit: International System of Unit (Système Internationale d'Unités; SI) (https://www.britannica.com/science/International-System-of-Units) should be used for all scientific and laboratory data.

References: Referring to references should be in the text by using reference numbers in parenthesis (i.e. [2]).

List of References: Publications cited in the text should only be presented in a list of references following the text of the manuscript. References should be listed according to their orders in which they are cited in the manuscript, i.e., [1] cited first, [2] cited next, and so on. An example of a reference list is below.

Examples:

[1] Berndt, T. (2002). "Friendship Quality and Social Development", ***Current Directions in Psychological Science***, vol.82, no.3, pp.114-140. **(Single authored article)**

[2] Rother, M. and Shook, J. (1999). "Learning to See: Value Stream Mapping to Create Value and Eliminate Muda", ***The Lean Enterprise Institute***, vol.22, no.4, pp.3-4**. (Multi-authored article)**

[3] Okamoto, G. (1999). ***Smart Antenna Systems and Wireless LANs,*** Boston: Kluwer Academic Publishers. **(Single Author Books)**

[4] Author, A. (Year). "Title of document", Retrieved from http://wwwwwwwwwwwwwwwwwwww wwwwwwwwwwwwwww (Access Date: 00.00.0000). **(Internet Sources)**

[5] Lastname, F.N. (Year). Title of dissertation (Doctoral dissertation). University Name, Institute Name, City. (Retrieved from Name of database). **(Published Dissertation)**

[6] Bergmann, P. G. (1993). Relativity, ***In The New Encyclopedia Britannica,*** (Vol. 26, pp. 501-508). Chicago, IL: Encyclopedia Britannica**.(Encyclopedia)**

[7] Author, A. A. (Year, Month Day). "Title of article", ***Title of Newspaper***. Retrieved from http://www.someaddress.com/full/url/wwwwwwwwwwwwwwwwwwwwwwwwwwwwwwwwwwwwww wwwwwwwwwww wwwwwwwwwwwwwww **(Newspaper article)**

[8] Önaçan, M.B.K., Uluağ, M., Önel, T. and Medeni, T.D. (2018). "Selection of Plagiarism Detection Software and Its Integration Into Moodle for Universities: An Example of Open Source Software Use in Developing Countries". Ricardo Queirós (ed.), Emerging Trends, Techniques, and Tools for Massive Open Online Course (MOOC) Management, ***IGI Global***, 250-265, pp. 255. **(Book chapter)**

Abbreviations and Acronyms: Standard abbreviations and acronyms should be used for each related discipline. Acronyms should be identified at the first occurrence in the text. Abbreviations and acronyms may also be attached to main text as an appendix.

Equations and Formulas: Equations and formulas should be numbered consecutively. These numbers must be shown within parentheses being aligned to right. In the text, equations and formulas should be referred with their numbers given in parentheses. Comprehensive formulas, not appropriate to be written in the texts, should be prepared in figures.

Figures and Tables: Figures and tables should be numbered consecutively. In the text referring to figures and tables should be made by typing "Figure 1" or "Table 1" etc. A suitable title should be assigned to each of them.

DENİZ BİLİMLERİ VE MÜHENDİSLİĞİ DERGİSİ (DBMD)
YAZIM KURALLARI

Genel Bilgiler: Yazılar; Microsoft Word'de tek satır aralığı ve iki yana yaslanarak hazırlanmalıdır. Yazı tipi: Times New Roman, 12 punto. Kenar boşlukları: sol 4,5 cm- sağ 3,5 cm- üst 5 cm- alt 7 cm- üst bilgi 3,25 cm- alt bilgi 6 cm, oluk 0. Kağıt ölçüsü: A4. Sayfa numaraları sayfanın alt ortasında -1-, -2-, -3- şeklinde yer almalıdır. Dipnot kullanılmamalıdır.

Yazı Yapısı: Yazı şu sırada hazırlanmalıdır: Başlık, Yazarlar, Özet, Anahtar Kelimeler, Başlık (Türkçe), Özet (Türkçe), Anahtar Kelimeler (Türkçe), Ana Metin, Ek (varsa), Referanslar.

Başlık: Başlık; açık, net, anlaşılır olmalı ve 15 kelimeyi geçmemelidir.

Öz (Abstract): Yazı, 100-200 kelimelik, arka plan, amaç, yöntem, bulgular ve sonuçtan oluşan yapılandırılmış bir özeti içermelidir.

Sayfa Sayısı: Dergiye gönderilecek yazıların boyutu, kaynakça dahil asgari 2000 kelime veya 5 sayfa, azami 7000 kelime veya 25 sayfa arasında olmalıdır.

Anahtar Kelimeler: Yazıyı sınıflandırmaya yarayacak, anahtar görevi yapan 3-5 kelime yer almalıdır.

Birimler: Yazının uluslararası alanlarda da kolay izlenebilir ve anlaşılabilir olması için Uluslararası Birim Sistemine (https://www.britannica.com/science/International-System-of-Units) uygun olarak hazırlanması gerekir.

Referans: Referanslar dipnotlar ile değil metin içinde açılacak parantezlerde yer alan referans numarası ile ([2] gibi) yapılmalıdır.

Referans Listesi: Makalenin ana metninden sonra sadece yazıda gönderme yapılan eserler yer almalıdır. Gönderme yapılan eserler, ana metin içerisinde atıf yapıldıkları sıraya göre listelenmelidir, yani ilk atıf yapılan eser [1], ikinci atıf yapılan eser [2] olmalı ve bu şekilde devam etmelidir. Bir referans listesi örneği aşağıdadır.

Örnekler:

[1] Berndt, T. (2002). "Friendship Quality and Social Development", ***Current Directions in Psychological Science***, vol.82, no.3, pp.114-140. **(Tek yazarlı makale)**

[2] Rother, M. and Shook, J. (1999). "Learning to See: Value Stream Mapping to Create Value and Eliminate Muda", ***The Lean Enterprise Institute***, vol.22, no.4, pp.3-4**. (Çok yazarlı makale);**

[3] Okamoto, G. (1999). ***Smart Antenna Systems and Wireless LANs,*** Boston: Kluwer Academic Publishers. **(Tek yazarlı kitap)**

[4] Author, A. (Year). "Title of document", Retrieved from http://wwwwwwwwwwwwwwwww wwwwwwww wwwwwwwwwww (Access Date: 00.00.0000). **(İnternet kaynakları)**

[5] Lastname, F.N. (Year). Title of dissertation (Doctoral dissertation). University Name, Institute Name, City. (Retrieved from Name of database). **(Yayınlanmış tez)**

[6] Bergmann, P. G. (1993). Relativity, ***In The New Encyclopedia Britannica,*** (Vol. 26, pp. 501-508). Chicago, IL: Encyclopedia Britannica**.(Ansiklopedi)**

[7] Author, A. A. (Year, Month Day). "Title of article", ***Title of Newspaper***. Retrieved from http://www.someaddress.com/full/url/wwwwwwwwwwwwwwwwwwwwwwwwwwwwwwwwwwwwwwwwwwww wwwwwwwwwwwwwwwwwwwwwwwwwwwwwww **(Gazete makalesi)**

[8] Önaçan, M.B.K., Uluağ, M., Önel, T. and Medeni, T.D. (2018). "Selection of Plagiarism Detection Software and Its Integration Into Moodle for Universities: An Example of Open Source Software Use in Developing Countries". Ricardo Queirós (ed.), Emerging Trends, Techniques, and Tools for Massive Open Online Course (MOOC) Management, ***IGI Global***, 250-265, pp. 255. **(Kitap bölümü)**

Notasyon ve Kısaltmalar: İlgili bilim alanının standart notasyon ve kısaltmaları kullanılmalı, yeni notasyonlar ise metin içinde ilk geçtiği yerde tanımlanmalıdır. Gerekli durumlarda, notasyon ve kısaltmalar ek olarak konulabilir.

Denklem ve Formüller: Denklem ve formüller ardışık olarak numaralandırılmalı ve bu numaralar sağa dayalı parantez içinde yazılmalıdır. Metin içinde denklem ve formüllere parantez içinde yazılan numaraları ile atıfta bulunulmalıdır. Metin arasında verilmesi uygun olmayan kapsamlı formüller şekil olarak hazırlanmalıdır.

Şekiller ve Tablolar: Şekiller ve tablolar, ardışık olarak numaralandırılmalıdır. Bunlara metin içinde "Şekil 1" veya "Tablo 1" şeklinde atıfta bulunulmalıdır. Her bir şekil ve tablo için uygun bir başlık kullanılmalıdır.

Publication Ethics and Responsibilities

Journal of Naval Sciences and Engineering (hereafter JNSE) is a peer reviewed, international, inter-disciplinary journal in science and technology, which is published semi-annually in November and April since 2003. JNSE it is committed to provide a platform where highest standards of publication ethics are the key aspect of the editorial and peer-review processes.

The editorial process for a manuscript to the JNSE consists of a double-blind review, which means that both the reviewer and author identities are concealed from the reviewers, and vice versa, throughout the review process. If the manuscrit is accepted in the review stage of the Editorial Process then, the submission goes through the editing stage, which consists of the processes of copyediting, language control, reference control, layout and proofreading. Reviewed articles are treated confidentially in JNSE.

Papers submitted to JNSE are screened for plagiarism with the iThenticate plagiarism detection tool. In case that the editors become aware of alleged or proven scientific misconduct, they can take the necessary steps. The editors have the right to retract an article whether submitted to JNSE or published in JNSE.

Following the completion of the editing stage, the manuscript is then scheduled for publication in an issue of the JNSE. The articles which are submitted to JNSE to be published are free of article submission, processing and publication charges. The accepted articles are published free-of-charge as online from the journal website and printed. The articles that are accepted to appear in the journal are made freely available to the public via the journal's website. The journal is also being printed by National Defense University Turkish Naval Academy Press on demand. The printed version can be accessed free of charge from the libraries of the Turkish Universities.

JNSE has editors and an editorial board which consists of academic members from at least five different universities. JNSE has an open access policy which means that all contents are freely available without charge to the user or his/her institution. Users are allowed to read, download, copy, distribute, print, search, or link to the full texts of the articles, or use them for any other lawful research purposes.
Publication ethics of the JNSE are mainly based on the guidelines and recommendations which are published by the Committee on Publication Ethics (COPE), World Federation of Engineering Organizations (WFEO), Council of Science Editors (CSE) and Elsevier's Publishing Ethics for Editors statements.
The duties and responsibilities of all parties in the publishing process including editors, authors and others are defined below.

The Responsibilities of the Authors:

-Authors are responsible for the scientific, contextual, and linguistic aspects of the articles which are published in the journal. The views expressed or implied in this publication, unless otherwise noted, should not be interpreted as official positions of the Institution.

-Authors should follow the "Author Guidelines" in JNSE's web page on DergiPark.

-Authors should conduct their researches in an ethical and responsible manner and follow all relevant legislation.

-Authors should take collective responsibility for their work and for the content of their publications.

-Authors should check their publications carefully at all stages to ensure that methods and findings are reported accurately.

-Authors must represent the work of others accurately in citations, quotations and references.

-Authors should carefully check calculations, data presentations, typescripts/submissions and proofs.

-Authors should present their conclusions and results honestly and without fabrication, falsification or inappropriate data manipulation. Research images should not be modified in a misleading way.

-Authors should describe their methods to present their findings clearly and unambiguously.

-Authors accept that the publisher of JNSE holds and retains the copyright of the published articles.

-Authors are responsible to obtain permission to include images, figures, etc. to appear in the article.

-In multi-authored publications - unless otherwise stated - author rankings are made according to their contributions.

-Authors should alert the editor promptly if they discover an error in any submitted.

-Authors should follow the publication requirements regarding that the submitted work is original and has not been published elsewhere in any language.

-Authors should work with the editor or publisher to correct their work promptly if errors are discovered after publication.

-If the work involves chemicals, procedures or equipment that have any unusual hazards inherent in their use, the authors must clearly identify these in the manuscript.

-If the work involves the use of animals or human participants, the authors should ensure that all procedures were performed in compliance with relevant laws and institutional guidelines and that the appropriate institutional committee(s) has approved them; the manuscript should contain a statement to this effect.

-Authors should also include a statement in the manuscript that informed consent was obtained for experimentation with human participants. Because the privacy rights of human participants must always be preserved. It is important that authors have an explicit statement explaining that informed consent has been obtained from human participants and the participants' rights have been observed.

-Authors have the responsibility of responding to the reviewers' comments promptly and cooperatively, in a point-by-point manner.

The Responsibilities of the Editors:

-Editors are responsible of enhancing the quality of the journal and supporting the authors in their effort to produce high quality research. Under no conditions do they allow plagiarism or scientific misconduct.

-Editors ensure that all submissions go through a double-blind review and other editorial procedures. All submissions are subject to a double-blind peer-review process and an editorial decision based on objective judgment.

-Each submission is assessed by the editor for suitability in the JNSE and then, sent to the at least two expert reviewers.

-Editors are responsible for seeking reviewers who do not have conflict of interest with the authors. A double-blind review assists the editor in making editorial decisions.

-Editors ensure that all the submitted studies have passed initial screening, plagiarism check, review and editing. In case the editors become aware of alleged or proven scientific misconduct, they can take the necessary steps. The editors have the right to retract an article. The editors are willing to publish errata, retractions or apologies when needed.

Yayın Etiği ve Sorumluluklar

Deniz Bilimleri ve Mühendisliği Dergisi (Bundan sonra DBMD olarak anılacaktır.); uluslararası düzeyde, hakemli, çok disiplinli, Nisan ve Kasım aylarında olmak üzere 2003 yılından bu yana yılda iki kez yayınlanan, bilim ve teknoloji dergisidir. DBMD yayın etiğinde en yüksek standartların, editoryal ve hakemlik süreçlerinin kilit unsuru olarak değerlendirildiği bir platform sunmayı taahhüt etmektedir.

DBMD'ne gönderilen her bir makale için değerlendirme sürecinde çift-kör hakemlik sistemi uygulanmaktadır. Buna göre, değerlendirme süreci boyunca hakem ve yazarlar birbirlerinin bilgilerini görememektedir. Dergiye gönderilen çalışmaların yazar-hakem ve hakem-yazar açısından süreçlerinde gizlilik esastır. DBMD'ne gönderilen makalelerin değerlendirme sürecindeki inceleme aşamasında kabul edilmeleri halinde, ilgili makaleler için düzenleme aşamasına geçilmektedir. Düzenleme aşamasında, ilgili makaleler yazım formatı ve dilbilgisel yönlerden incelenir. Makalelerin sayfalar üzerindeki biçimi ve yerleşimleri kontrol edilip düzenlenir. Ayrıca referans kontrolü yapılır. DBMD'nde kontrol edilen ve düzenlenen makaleler gizli tutulmaktadır.

DBMD'ne gönderilen makaleler, iThenticate intihal tespit programı aracılığıyla bilimsel çalıntı konusunda kontrol edilir. Editörler, iddia edilen veya kanıtlanmış bir bilimsel kötü kullanımdan ya da usulsüzlükten haberdar olurlarsa bu konuda gerekli adımları atabilirler. Bu anlamda, Editörler gerekli durumlarda DBMD'ne gönderilen ya da DBMD'nde yayınlanmış makaleleri geri çekme hakkına sahiptir.

Düzenleme aşamasının başarılı olarak sonuçlanmasını takiben, ilgili makaleler DBMD'nin bir sayısında yayınlanmak üzere saklı tutulur ve kayıt altına alınır. DBMD'ne yayınlanmak üzere gönderilen makaleler; yazılı materyal gönderme, işleme ve yayınlama süreçlerindeki tüm ücretlerden muaf tutulmaktadır. DBMD'nde yayınlanmak üzere kabul edilen makaleler, derginin internet sitesinden çevrimiçi olarak ücretsiz bir şekilde yayınlanır ve basılır. Dergide yayınlanması kabul edilen çalışmalar, derginin web sitesinden açık erişim ile erişilebilir kılınmıştır. Dergi ayrıca, Milli Savunma Üniversitesi, Deniz Harp Okulu Basımevi tarafından basılmaktadır. Derginin basılı haline Üniversite kütüphanelerinden erişilebilmektedir.

DBMD; editörü ve en az beş değişik üniversitenin öğretim üyelerinden oluşmuş danışman grubu ile açık erişim politikasını benimsemektedir. Buna göre, tüm içerikler ücretsiz olarak kullanıcılar veya kurumlar için ulaşılabilirdir. Kullanıcıların DBMD bünyesindeki makalelerin tam metinlerini okuma, indirme, kopyalama, dağıtma, yazdırma, arama veya bunlara bağlantı verme ve diğer yasal araştırma amaçları için kullanma hakları saklı tutulmaktadır.

DBMD'nin yayın etiği, temel olarak Yayın Etiği Komitesi (COPE), Dünya Mühendislik Kuruluşları Federasyonu (WFEO), Bilim Kurulu Editörleri (CSE) ve Elsevier'in Editörler için Yayın Etiği açıklamaları kapsamında yayınlanmış yönergelere ve önerilere dayanmaktadır.

Editörler, yazarlar ve diğer taraflar da dahil edilebilecek şekilde yayın sürecindeki görev ve sorumluluklar aşağıdaki gibi tanımlanmıştır.

Yazarların Sorumlulukları:

-Yazarlar, dergide yayınlanan makalelerinin bilimsel, bağlamsal ve dilsel yönlerinden sorumlu tutulmaktadır. Dergide ifade edilen veya ima edilen görüşler, aksi belirtilmediği sürece, Enstitünün resmi görüşü olarak yorumlanamaz ve yansıtılamaz.

-Yazarlar çalışmalarında, DBMD'nin DergiPark internet sayfasında yer alan "Yazım Kuralları"nı dikkate almalıdır.

-Yazarlar araştırmalarını etik ve sorumlu bir şekilde yürütmeli ve ilgili tüm mevzuatları takip etmelidir.

-Yazarlar çalışmaları ve yayınlarının içeriği için ortak sorumluluk almalıdır.

-Yazarlar, yöntemlerin ve bulguların doğru bir şekilde raporlandığından emin olmak için yayınlarını her aşamada dikkatlice kontrol etmelidir.

-Yazarlar, başkalarına ait çalışmaları dolaylı alıntı, doğrudan alıntı ve referanslar ile doğru bir şekilde göstermelidir. Yazarlar, makalelerindeki fikirlerin şekillendirilmesinde etkili ya da bilgilendirici olmuş her türlü kaynağa referans vermelidir.

-Yazarlar çalışmalarındaki hesaplamaları, ispatları, veri sunumlarını ve yazı tiplerini dikkatlice kontrol etmelidir.

-Yazarlar çalışmalarının sonuçlarını dürüstçe; uydurma, çarpıtma, tahrifat veya uygunsuz manipülasyona yer vermeden sunmalıdır. Çalışmalardaki görsel kaynaklar yanıltıcı bir şekilde değiştirilmemelidir.

-Yazarlar, çalışmalarındaki bulguları açık ve net bir şekilde sunmak için araştırma yöntemlerini tanımlamalı ve paylaşmalıdır.

-Yazarlar, yayınlanmış makalelerinin telif haklarını DBMD yayıncısına devrettiklerini kabul etmektedir.

-Yazarlar çalışmalarına çeşitli görsel kaynakları, figürleri, şekilleri vb. dahil etmek için gerekli izinleri almakla yükümlüdür. İlgili çalışmada yer alması gereken resim, şekil vb. anlatımı destekleyici materyaller için gerekli kişilerden ya da kurumlardan izin alınması yazarın sorumluluğundadır.

-Çok yazarlı yayınlarda -aksi belirtilmedikçe- yazar sıralamaları sunulan katkılara göre yapılmalıdır.

-Yazarlar gönderdikleri çalışmada herhangi bir hata tespit ederlerse bu konuda derhal editörü uyarmalıdır.

-Yazarlar dergiye gönderdikleri makalelerin başka bir yerde yayımlanmamış ya da yayımlanmak üzere gönderilmemiş olmaları ile ilgili DBMD'nin DergiPark internet sayfasında yer alan "Yayın Kuralları"nı dikkate almalıdır.

-Yazarlar, ilgili çalışmaları DBMD'nde yayınlandıktan sonra hata tespit ederlerse bu konuda gerekli düzeltmelerin yapılabilmesi amacıyla derhal editör veya yayıncı ile iletişime geçip onlar ile birlikte çalışmalıdır.

-İlgili çalışmada, doğası gereği kullanımlarında olağandışı tehlikeler barındıran çeşitli kimyasallar veya ekipmanlardan yararlanılmış ise yazarların tüm bunları çalışmasında açıkça belirtmesi ve tanımlaması gerekmektedir.

-İnsanlar ve hayvanların katılımını gerektiren çalışmalar için, yazarlar tüm sürecin ilgili yasalara ve kurumsal yönergelere uygun olarak gerçekleştirildiğinden emin olmalıdır ve ilgili komitelerden etik onay alındığını çalışmalarında açık bir şekilde ifade edip belgelendirmelidir.

-İnsanların katılımını gerektiren çalışmalar için, yazarlar kurumsal etik kurul onayı almakla yükümlüdürler. Yazarlar, katılımcıların süreç ile ilgili olarak bilgilendirildiklerini ve bu anlamda, katılımcılardan gerekli izinlerin alındığını bildirmek ve belgelemek zorundadır. Yazarlar, katılımcıların haklarının gözetildiğini açıklayan açık bir bildirim sunmalıdır. Ayrıca bu süreçte, katılımcıların gizlilik hakları her zaman korunmalıdır.

-Yazarlar, hakemlerin değerlendirmelerini, yorumlarını ve eleştirilerini zamanında ve işbirliği içerisinde dikkate almalıdır ve bu konuda, gerekli güncellemeleri yapmalıdır.

Editörlerin Sorumlulukları:

-Editörler, derginin bilimsel kalitesini arttırmak ve yazarları bilimsel kalitesi yüksek araştırmalar üretmek için desteklemek ile sorumludur. Hiçbir koşulda, intihal ya da bilimsel kötüye kullanıma izin verilmemektedir.

-Editörler, dergiye gönderilen her çalışmanın çift-kör hakemlik sürecine ve diğer editoryal süreçlere tabi olmasını sağlamaktadır. DBMD'ne gönderilen her çalışma, çift-kör hakemlik sürecine ve nesnel değerlendirmeye dayalı editör kararına bağlı tutulmaktadır.

-DBMD'ne gönderilen her bir çalışma, uygunlukları açısından editör tarafından değerlendirilir ve daha sonrasında, incelenmesi ve değerlendirilmesi amacıyla en az iki uzman hakeme gönderilir.

-Editörler, yazarlar ile çıkar çatışması olmayan hakemleri, çalışmayı değerlendirmek üzere atamakla sorumludur. Çift-kör hakemlik süreci, editör için değerlendirme ve düzenleme aşamalarında katkı sağlamaktadır.

-Editörler, DBMD'ne gönderilen tüm çalışmaların ön kontrol, tarama, intihal kontrolü, değerlendirme ve düzenleme aşamalarından geçmesini sağlar. Editörler iddia edilen veya kanıtlanmış bilimsel kötü kullanımdan haberdar olurlarsa makaleyi geri çekebilirler. Editörler, gerekli durumlarda gönderilen çalışmayı düzeltme, geri çekme veya çalışma hakkında özür yayınlama hakkına sahiptir.

NATIONAL DEFENSE UNIVERSITY
BARBAROS NAVAL SCIENCES AND ENGINEERING INSTITUTE
JOURNAL OF NAVAL SCIENCES AND ENGINEERING

VOLUME: 16 NUMBER: 1 APRIL 2020 ISSN: 1304-2025

CONTENTS / İÇİNDEKİLER

MİLLİ SAVUNMA ÜNİVERSİTESİ
BARBAROS DENİZ BİLİMLERİ VE MÜHENDİSLİĞİ ENSTİTÜSÜ
DENİZ BİLİMLERİ VE MÜHENDİSLİĞİ DERGİSİ

CİLT: 16 SAYI: 1 NİSAN 2020 ISSN: 1304-2025